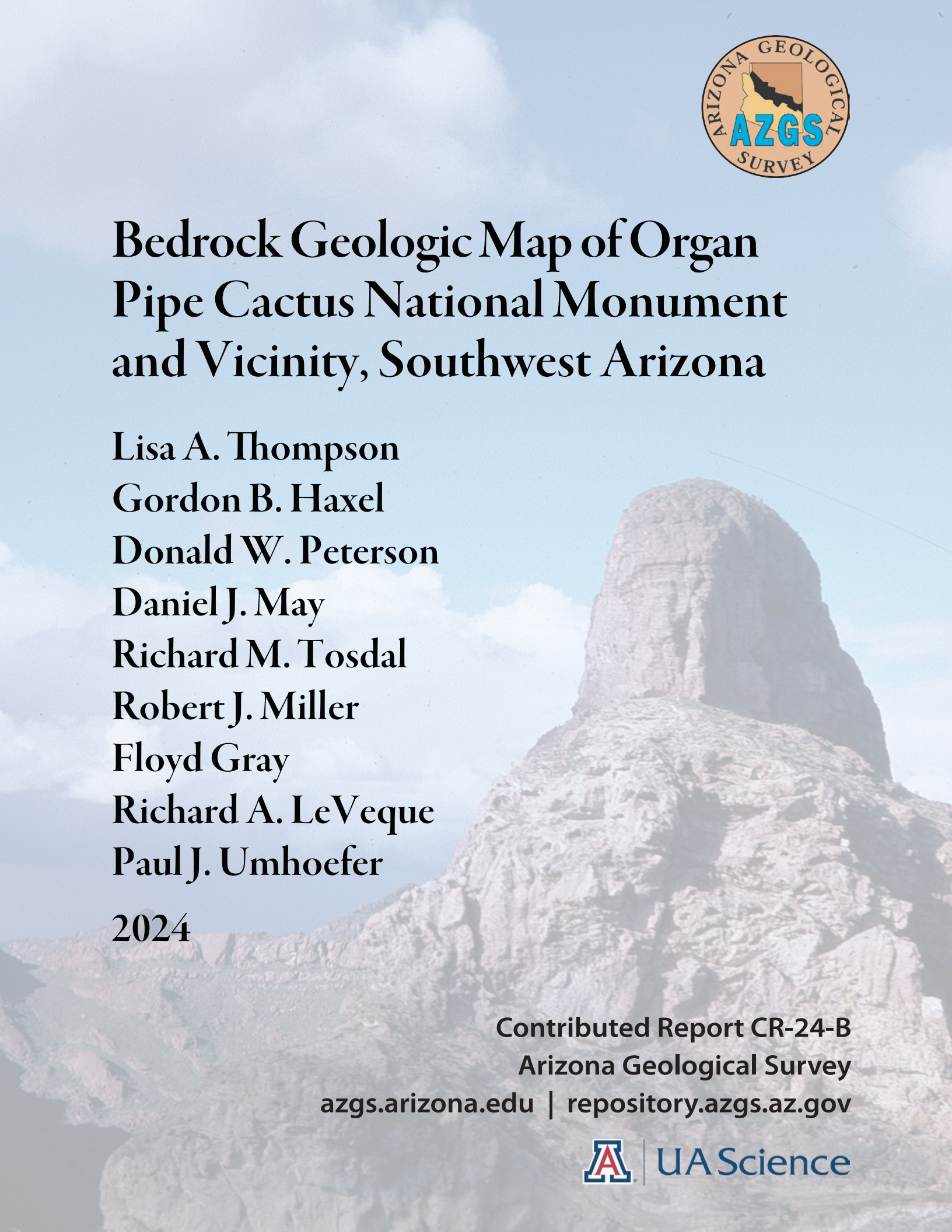


Bedrock Geologic Map of Organ Pipe Cactus National Monument and Vicinity, Southwest Arizona

Lisa A. Thompson
Gordon B. Haxel
Donald W. Peterson
Daniel J. May
Richard M. Tosdal
Robert J. Miller
Floyd Gray
Richard A. LeVeque
Paul J. Umhoefer

2024

Contributed Report CR-24-B
Arizona Geological Survey
azgs.arizona.edu | repository.azgs.az.gov

UA Science

Arizona Geological Survey

P.A. Pearthree, Arizona State Geologist and Director

Manuscript approved for publication October 2023
Printed by the Arizona Geological Survey
All rights reserved

For an electronic copy of this publication: www.repository.azgs.az.gov

For information on the mission, objectives or geologic products of the Arizona Geological Survey visit azgs.arizona.edu

This publication was prepared by the Arizona Geological Survey at the University of Arizona. The University of Arizona, or any department thereof, or any of their employees, makes no warranty, expressed or implied, or assumes any legal liability or responsibility for the accuracy, completeness, or usefulness of any information, apparatus, product, or process disclosed in this report. Any use of trade, product, or firm names in this publication is for descriptive purposes only and does not imply endorsement by the University of Arizona or the U.S. Government.

The AZGS Contributed Report series provides non-AZGS authors with a forum for publishing documents concerning Arizona geology. The Arizona Geological Survey issues no warranty, expressed or implied, regarding the suitability of this product for a particular use. Moreover, the Arizona Geological Survey shall not be liable under any circumstances for any direct, indirect, special, incidental, or consequential damages with respect to claims by users of this product.

Citation:

Thompson, L.A., Haxel, G.B., Peterson, D.W., May, D.J., Tosdal, R.M., Miller, R.J.,Gray, F., LeVeque, R.A., and Umhoefer, P.J., 2024, Geologic map of Organ Pipe Cactus National Monument and vicinity, southwest Arizona: Arizona Geological Survey Contributed Report CR-24-B, 28 p., scale 1:40,000.

Cover image: Diaz Spire, Ajo Range, Organ Pipe Cactus National Monument: Miocene latite.

UA SCIENCE
ARIZONA GEOLOGICAL SURVEY
Geosciences serving Arizona since 1887

Bedrock Geologic Map of Organ Pipe Cactus National Monument and Vicinity, Southwest Arizona
2024

Lisa A. Thompson[1,2]
Gordon B. Haxel[2,3,4]
Donald W. Peterson[4] (1924–2003)
Daniel J. May[4]
Richard M. Tosdal[4]
Robert J. Miller[4]
Floyd Gray[4]
Richard A. LeVeque[4]
Paul J. Umhoefer[2] (1955–2021)

Present or recent affiliations

[1]Arizona Geological Survey, University of Arizona, Tucson, Arizona
[2]Division of Geosciences, School of Earth and Sustainability, Northern Arizona University, Flagstaff, Arizona
[3]U.S. Geological Survey, Flagstaff, Arizona

Affiliation at time of geologic mapping, ca. 1980

[4]U.S. Geological Survey, Menlo Park, California

Arizona Geological Survey Contributed Report CR-24-B

Produced by LAT and GBH, using Adobe InDesign CS6
Text: Garamond Pro Medium 11/13
Captions: Myriad Pro Semicondensed 10/12

CONTENTS

Introduction: Organ Pipe Cactus National Monument 1

Geologic Mapping of Organ Pipe Cactus National Monument and Vicinity 1

Regional Geologic History and Overview of Major Rock Units 4

- Proterozoic: Consolidation of Continental Crust 4
- Early and Middle Paleozoic: Transgression of Shallow Seas 4
- Middle to Late Jurassic: Arc and Extensional Magmatism 5
- Late Cretaceous and Early Paleogene: Granitoid Plutonism, Thrust Faulting, and Regional Metamorphism 7
- Late Oligocene to Miocene: Volcanism and Crustal Extension 8
- Late Neogene to Present: Aggradation and Incision 9

Description of Map Units 9

- Quaternary Surficial Deposits 10
- Neogene and Paleogene Rocks, Largely Volcanic 10
  - • Batamote andesite complex (middle Miocene, units Nb) 10
  - • Montezuma Head rhyolite (early Miocene, units Nm) 11
  - • Childs Latite and coeval plutonic rocks (early Miocene, units Nc) 12
  - • Pinkley Peak rhyolite (early Miocene, units Np) 14
  - • Miscellaneous igneous and sedimentary rocks 16
- Late Cretaceous to Early Paleogene Chagit Vo gneiss 15
- Late Cretaceous Leucocratic Granites 16
- Late Cretaceous Plutonic and Volcanic Rocks 18
- Latest Jurassic Conglomerate 20
- Late Jurassic Intrusive Rocks 21
- La Abra complex; Middle and Late Jurassic Igneous and Sedimentary Protoliths, Late Cretaceous to Early Paleogene Metamorphism 21
- Paleozoic Sedimentary and Metasedimentary Rocks 23
- Paleoproterozoic Igneous and Metamorphic Rocks 24

Acknowledgments 25

References Cited 25

FIGURES

1 Location map, Organ Pipe Cactus National Monument (OPCNM), southwest Arizona 1
2 Geographic features of OPCNM 2
3 Columnar summary of geologic history 3
4 Index to geologic mapping 4
5 Age and correlation of map units 5
6 Quitobaquito thrust, Quitobaquito Hills 8
7 Tectonic sheets and mylonitic shear zone, northern Puerto Blanco Mountains 9
8 Ajo volcanic field 9
9 Batemote andesite complex, Bates Mountains 10
10 Montezuma Head rhyolite, Ajo Range 11
11 Childs Latite: lavas flows, megacrystic phenocrysts 13
12 Composition of Late Cretaceous granitoids 18
13 Senita Basin granite, Sonoyta Mountains 19
14 Columnar biotite, Bandeja Well granodiorite 19
15 Latest Jurassic metaconglomerate 20
16 Latest Jurassic limestone-clast conglomerate; gastropod fossil hash 20
17 Metamorphosed quartz porphyry, northern Puerto Blanco Mountains 23
18 Metamorphosed Pozo Nuevo granite porphyry, Quitobaquito Hills 23
19 Mylonite derived from Pozo Nuevo granite porphyry 24
20 Cambrian strata, latest Jurassic conglomerate, latest Cretaceous granodiorite 24
21 Wollastonite in contact-metamorphic Paleozoic limestone 25

TABLES

1 Isotopic ages 6
2 Whole-rock analyses, Late Cretaceous plutonic rocks 17
3 Whole-rock analyses, Jurassic igneous rocks 22

PLATE

Bedrock geologic map of Organ Pipe Cactus National Monument and vicinity, southwest Arizona; scale 1:40,000

INTRODUCTION: ORGAN PIPE CACTUS NATIONAL MONUMENT

Organ Pipe Cactus National Monument (OPCNM; Figs. 1, 2) preserves an area of 1300 km² typical of the Lower Sonoran Desert ecosystem of southern Arizona, encompasses part of the ancestral lands of the Tohono O'odham Nation, and adjoins the international border between United States and Mexico (Laird et al., 1997; Felger et al., 2007; Dimmitt et al., 2015; KellerLynn, 2022). In 1976, the Monument was declared a UNESCO Biosphere Reserve; in 1977, 95 percent of the Monument area was designated Wilderness. The hallmark species of OPCNM is the organpipe cactus (*Stenocereus thurberi*). This columnar cactus, though common in northwest Mexico and widely scattered through parts of southwest Arizona, is most abundant in the United States in OPCNM (Turner et al., 1995). Another arboreal Mexican cactus, the senita (*Lophocereus schottii*), is found in the U.S. only in one small area within OPCNM.

OPCNM geology is characterized by northwest-southeast trending mountain ranges separated by broad alluvial plains, typical of the southern Basin and Range tectonic province. Diverse volcanic, intrusive, metamorphic, and sedimentary rocks exposed within and near the Monument record nearly two billion years of Earth history (Fig. 3), weather to picturesque geomorphic features, and support several distinctive plant communities (Felger et al., 1992). Rocks near the town of Ajo (18 km north of the Monument) host ores of copper, molybdenum, and gold.

This report is a much-revised version of data originally compiled for the National Park Service Geologic Resource Inventory (Skinner et al., 2008). The report and accompanying map collect decades-long work in geologic mapping of OPCNM and analytical studies of its rocks; document the geologic history of the Monument; and provide a complete, current geologic map for scientific, educational, and public use.

GEOLOGIC MAPPING OF ORGAN PIPE CACTUS NATIONAL MONUMENT AND VICINITY

In late 1970s and early 1980s, geologists of the U.S. Geological Survey (USGS) undertook geologic mapping of a large region

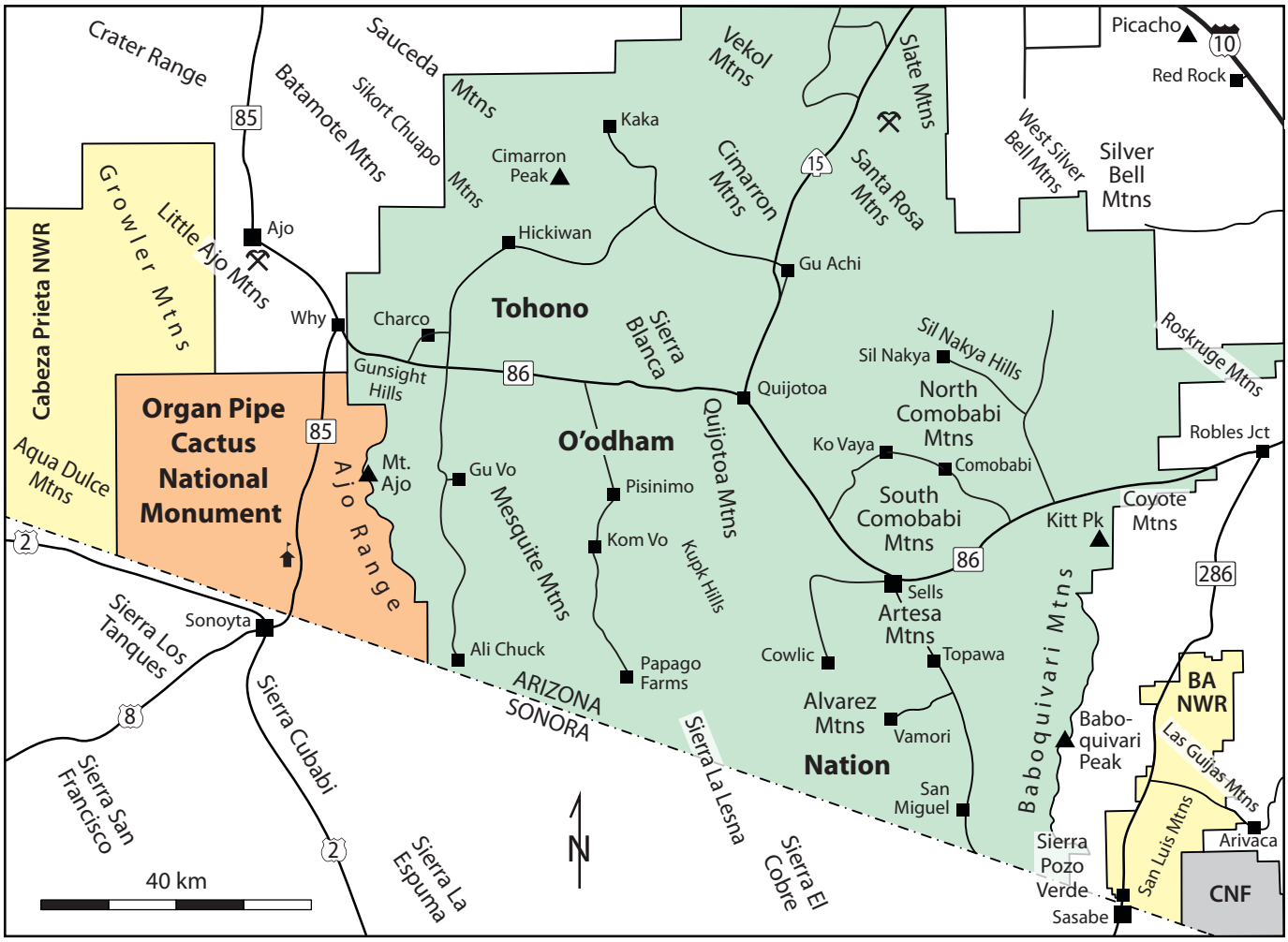


Figure 1. Organ Pipe Cactus National Monument (OPCNM) and surrounding region, southwest and south-central Arizona, showing geographic names mentioned in text. See Figure 2 for geographic names in OPCNM and vicinity. NWR, National Wildlife Refuge; BA NWR, Buenos Aires NWR; CNF, Coronado National Forest.

(~ 5300 km²) of southwest and south-central Arizona, including the Ajo and Lukeville 2°-by-1° quadrangles (Gray et al., 1988) and Tohono O'odham (then Papago) Indian Reservation (Beikman et al., 1995). Helicopter-supported geologic mapping of OPCNM and vicinity was conducted primarily in February and March 1980, by the second through seventh authors of this report (Fig. 4). Most mapping was done on stereo pairs of black-and-white aerial photographs, scale ≈ 1:30,000.

Upon completion of mapping, Peterson was designated to oversee compilation and publication. This plan was upset by the eruption of Mt. St. Helens (Washington) in May 1980. Peterson, who had previously been Scientist-in-Charge of the USGS Hawaiian Volcano Observatory, was selected to organize and lead a new Cascades Volcano Observatory, in Vancouver. Thus was the Organ Pipe geologic map deprived of its advocate and facilitator. By 1981 or 1982 the other six mappers likewise had either moved on to other projects and responsibilities or returned to graduate school, so the 1980 field mapping was never fully compiled. Nonetheless, parts of it were incorporated into maps, papers, and abstracts by

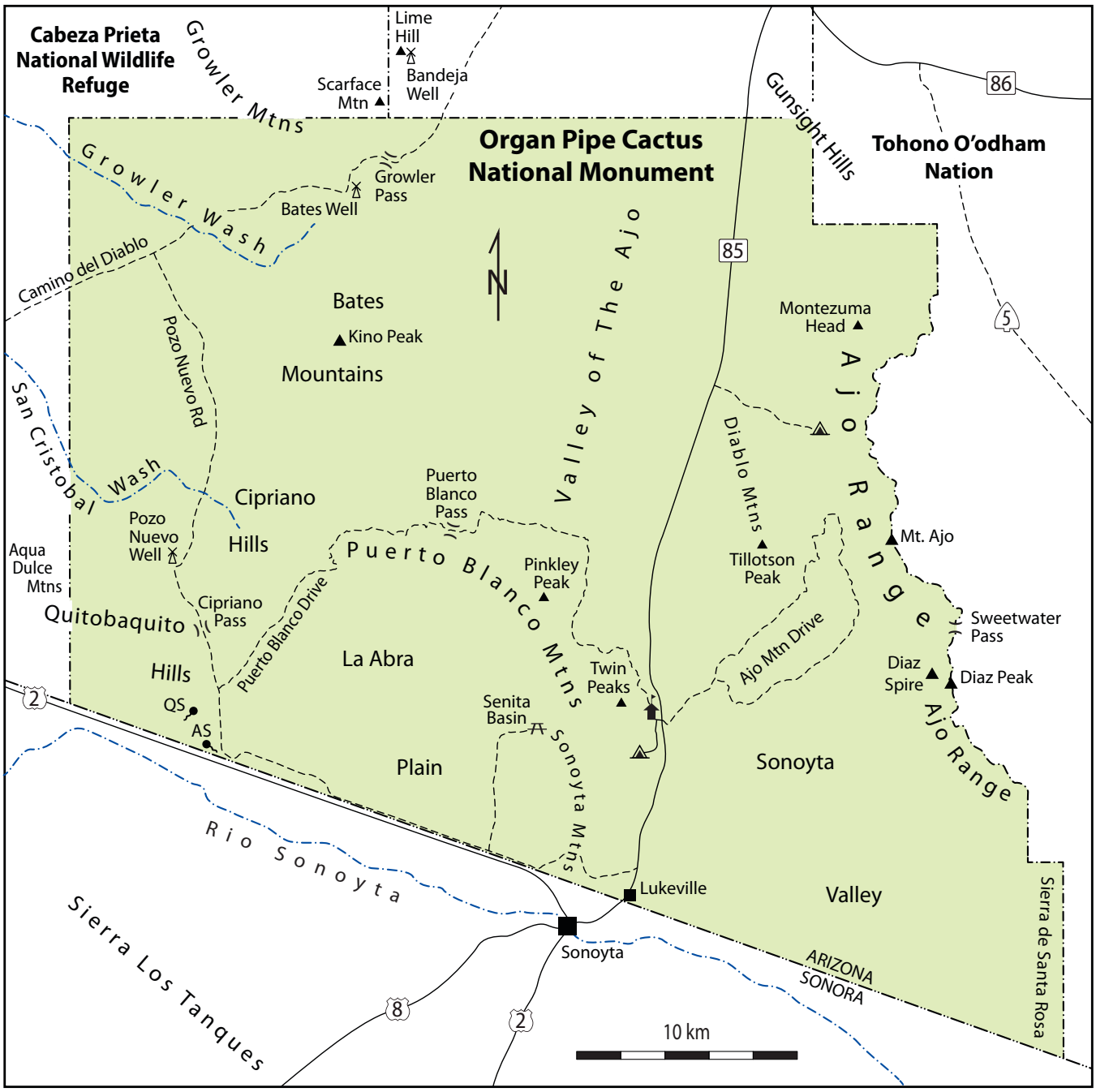


Figure 2. Geographic features of Organ Pipe Cactus National Monument (KellerLynn, 2022) and vicinity (Fig. 1). AS, Aquajita Spring; QS, Quitobaquito Springs. Natural distribution of the senita cactus (*Lophocereus schottii*) in the United States is restricted to the area around Senita Basin.

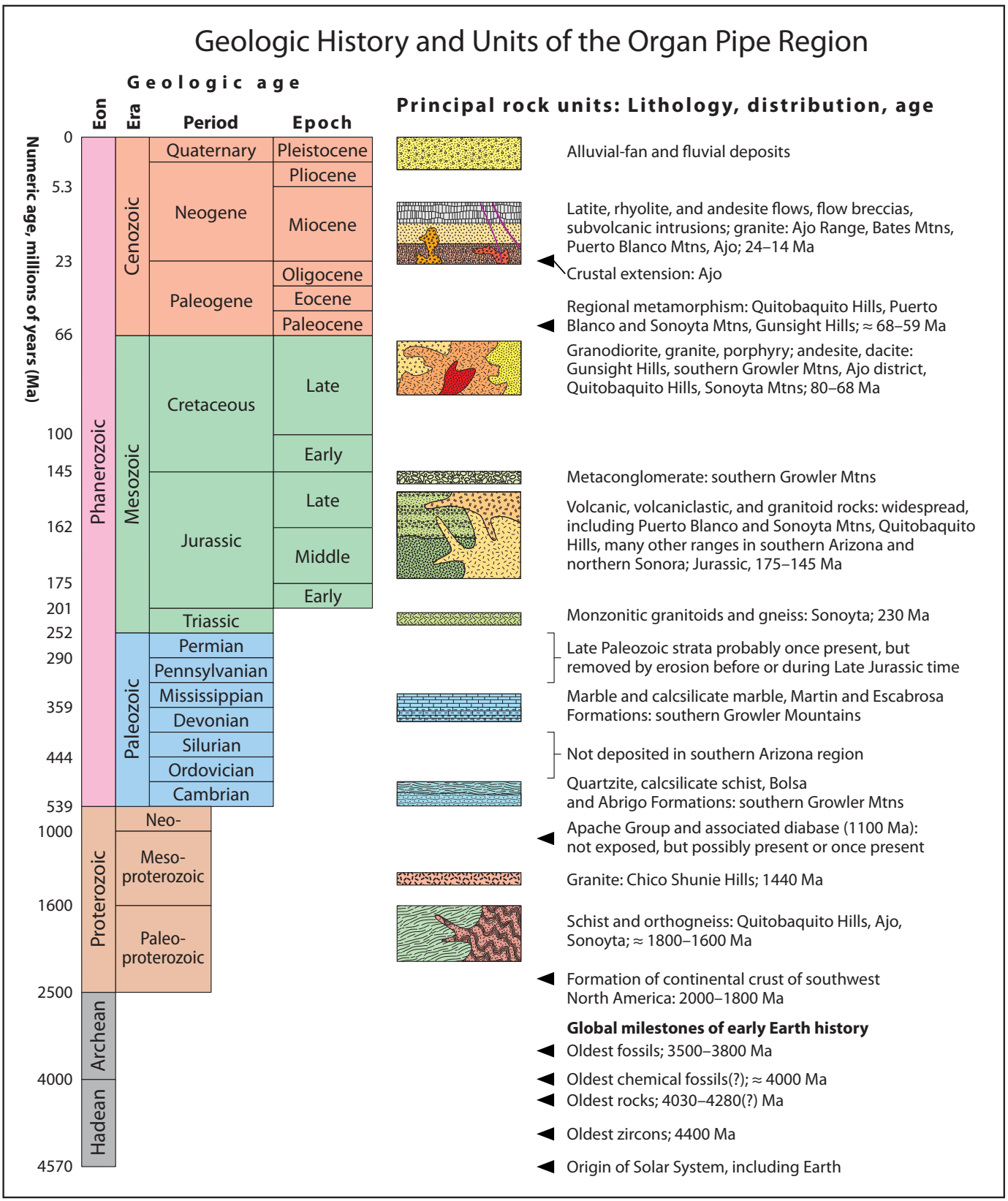


Figure 3. Columnar summary of geologic history of Organ Pipe Cactus National Monument (OPCNM) region, southwest Arizona and northwest Sonora (c.f. Fig. 5). Region included (Fig. 1) is approximately OPCNM (Fig. 2); Sierra Los Tanques and Sonoyta area; Agua Dulce, Growler, Little Ajo, and Batamote Mountains; Ajo district; and western Tohono O'odham Nation.

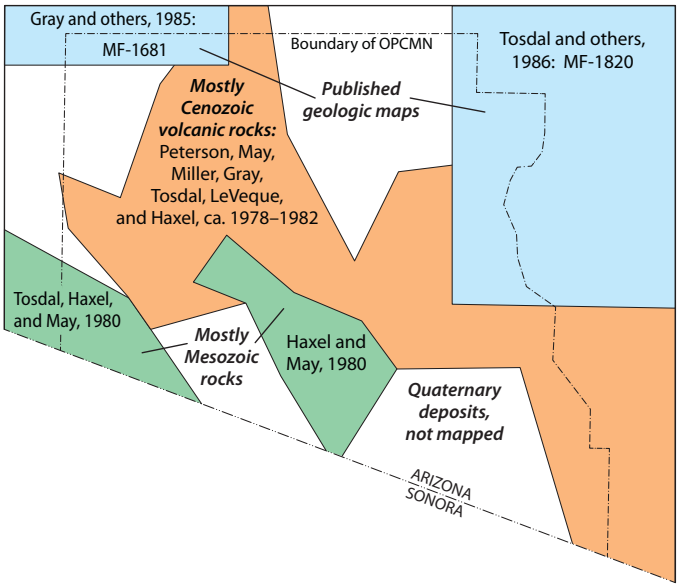


Figure 4. Index to geologic mapping. Blue rectangles, published geologic maps; vermilion and green polygons, mapping compiled in Plate 1; white polygons, Quaternary deposits, not individually mapped.

May et al. (1981), Gray and Miller (1984a, b), Haxel et al. (1984), Gray et al. (1985, 1988), Tosdal et al. (1986, 1989, 1990), Brown (1992), Beikman et al. (1995), and Bezy et al. (2000).

Circa 1983, a contract was issued to an independent geologist for compilation of the OPCMN mapping, but funding shortfall prevented completion. Sometime in the interval 1985–1995, that partial compilation was digitized by the National Park Service (NPS), but never published.

In 2006, Thompson (née Skinner) and Umhoefer, Northern Arizona University, were contracted by the NPS to complete the OPCMN geologic map (Skinner et al., 2008). They recompiled original mapping from aerial photographs, paper maps, and field notes. Field maps were scanned, georectified, and digitized; areas lacking coverage were digitized from Gray et al. (1985, 1988) and Tosdal et al. (1986). Lithologic descriptions were generated from field notes and several hundred thin sections. This map was then edited by several NPS personnel, including T. Connors, B. Heise, C. McCoy, S. O'Meara, and P. Reiker.

In 2022–2024, the final geologic map accompanying this report was revised from the 2008 NPS data, with further contributions by Haxel. The map undoubtedly has local inaccuracies owing to its convoluted compilation history and the need to work with decades-old folded paper field maps. Positional errors could locally be as large as 50 m. Moreover, Thompson, who compiled all the digital data, was not one of the original field mappers. In addition to these issues with the map itself, some map-unit information has been lost over the four decades from field mapping to publication; hence some lithologic descriptions are more detailed than others. Despite these minor limitations, this map and report (along with more recent studies by Rossi, 2022; Rossi et al., 2023) represent the current state of geologic knowledge of Organ Pipe Cactus National Monument and vicinity. The map complements a recent NPS *Geologic Resources Inventory Report* for OPCNM by Katie KellerLynn (2022).

REGIONAL GEOLOGIC HISTORY AND OVERVIEW OF MAJOR ROCK UNITS

Six principal tectonic episodes shaped the geologic framework of the OPCNM region (Figs. 3, 5): (1) Early to Middle Proterozoic crust formation; (2) Paleozoic deposition of cratonal sedimentary strata; (3) Jurassic magmatism and crustal extension; (4) Late Cretaceous and Paleogene plutonism, contractional deformation, and regional metamorphism; (5) late Oligocene to Miocene extension and volcanism; and (6) Pliocene to Holocene aggradation and incision of alluvial sediment.

Proterozoic: Consolidation of Continental Crust

The continental crust of southwest North America formed and was consolidated in Paleoproterozoic time (Karlstrom and Bowring, 1988; Meijer, 2014; Blakey and Ranney, 2018). These early episodes are very sparsely represented in the rock record of the OPCNM region, by small areas of Pinal Schist (unit Xp) and two types of gneiss (units Xg, Xo). The more extensive of the gneiss units is ≈ 1640 Ma (Table 1; Rossi, 2022; Rossi et al., 2023). Pinal Schist is a local instance of a unit widespread in southern Arizona (Meijer, 2014), but regional relations of the gneisses are unknown. Paleoproterozoic igneous and meta-igneous rocks are better characterized in northwest Sonora, where U-Pb ages are typically 1.8–1.6 Ga (e.g., Anderson and Silver, 2005; Nourse et al., 2005).

Two subsequent episodes of crustal evolution in Mesoproterozoic time affected much of southern Arizona, but are only minor aspects of the geologic record of the OPCNM region. The first was widespread granitic plutonism, ≈ 1.4 Ga (Anderson, 1989). This episode is represented locally by the Chico Shunie Granite, 1.44 Ga, in the Ajo district, ≈ 10 km north of the map area (Gilluly, 1946; Gray et al., 1988). The second Mesoproterozoic episode, ca. 1.1 Ga, was rifting to form basins filled by sedimentary strata of the Apache Group, closely followed by intrusion of diabase (Wrucke, 1989). Exposures of the Apache Group and associated diabase nearest OPCNM are in the Vekol and Slate Mountains, 100 km northeast (Fig. 1; Beikman et al., 1995). If Apache Group strata were deposited in the OPCMN region, they are now either buried or removed by erosion.

Early to Middle Paleozoic: Transgression of Shallow Seas

By Cambrian time, the Arizona Proterozoic craton had become a platform for passive-margin sedimentation (Beus, 1989; Dickinson, 1989; Middleton, 1989; Łabaj and Pratt, 2016). Numerous transgressive and regressive episodes through early Paleozoic time deposited shallow marine, marginal marine,

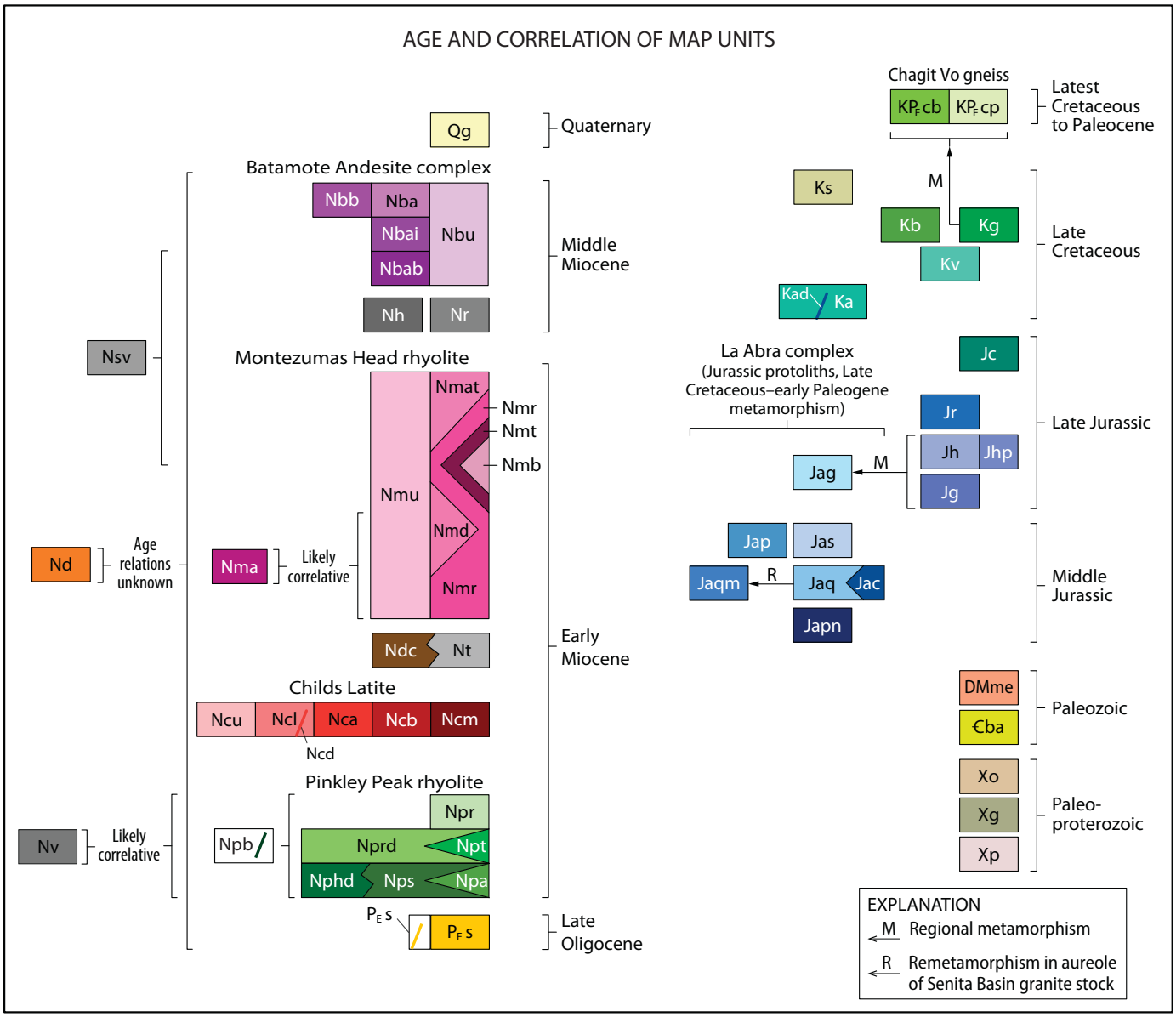


Figure 5. Age and correlation of map units (c.f. Fig. 3). Dikes shown as boxes where their lithic designator is different from that of the host map unit. Dikes shown as lines where their map color is different from the host map unit.

fluvial, and eolian sediments, which together constitute the sedimentary section well known from the Grand Canyon of northern Arizona (Beus and Morales, 2003). Paleozoic cratonal strata undoubtedly once blanketed the OPCMN region (McKee, 1947), but have been almost entirely removed by Mesozoic and/or Cenozoic erosion. Within the map area, remnants of four Paleozoic units—Cambrian Bolsa Quartzite and Abrigo Formation (combined as map unit Cba), Devonian Martin Formation and Mississippian Escabrosa Limestone (combined as unit DMme)—are exposed in two small areas (see map unit descriptions). In the larger of the two outcrop areas, Paleozoic rocks have been converted to wollastonite-bearing skarn by latest Cretaceous contact metamorphism.

Paleozoic rocks are sparse in south-central and southwest Arizona and adjacent Sonora (Richard et al., 2000; Anderson et al., 2005a, b; Haxel et al., 1980b, 2008a). Intact, unmetamorphosed lower Paleozoic sections nearest to OPCMN are in the Vekol and Slate Mountains (Fig. 1; Blacet et al., 1978; Dockter et al., 1978; Beikman et al., 1995). These sections include Pennsylvanian strata, of which no trace remains in the OPCNM region. Well-documented Paleozoic rocks in the Coyote Mountains (Fig. 1; Carrigan, 1971; Haxel et al., 1980a, 2008b) were, before metamorphism, comparable to those in the map area.

Middle to Late Jurassic: Arc and Extensional Magmatism

In latest Permian through Triassic time, the continental margin of southwest North America progressed from passive to active and was then dominated by subduction-related magmatism

(Blakey and Ranney, 2018). Triassic igneous rocks and derivative gneiss crop out in a few localities around OPCNM (e.g., Campbell and Anderson, 2003) but none are known to be exposed within the map area.

By Jurassic time, a broad magmatic arc had developed across southwest North America (Tosdal et al., 1989; Tosdal and Wooden, 2015; Busby and Centeno-García, 2022). The extensive Middle and Late Jurassic igneous rocks of OPCNM represent the first geologic episode well recorded in the rocks of the region, and they form most of the crystalline substrate upon which the more-prominent Miocene volcanic rocks of the Monument rest. Within this Jurassic foundation terrane, two related Middle Jurassic rock units are most voluminous and central in importance: the volcanic and subvolcanic quartz porphyry (unit Jaq) and the epizonal Pozo Nuevo granite porphyry (unit Japn). (See note at beginning of Description of Map Units regarding informal geologic names.) These units make up much of the La Abra complex (seven map units prefixed by Ja; Fig. 5), widespread in the Puerto Blanco and Sonoyta Mountains, and northern Quitobaquito Hills.

Age(s) of the quartz porphyry and Pozo Nuevo granite porphyry are ≈ 172 Ma (Table 1; Rossi, 2022; Rossi et al., 2023). Similar silicic igneous rocks, approximately the same age, are widespread in south-central Arizona and north-central Sonora,

Table 1. Representative K-Ar and U-Pb isotopic ages for geologic units within the map area. Map number: sample localities plotted on Plate 1. Materials: bio, biotite; san, sanidine; wr, whole rock; zir, zircon.

Map number	Sample	Type	Material	Age ± uncertainty (Ma)	Reference	Latitude	Longitude	Datum[1]
Batamote andesite complex (unit Nba)								
		K-Ar		14.4 ± 0.7	Skinner, 2008			
1	109	K-Ar	wr	15.0 ± 2.2	Eberly and Stanley, 1978	32.3056	–113.0072	NAD27
2	2114	K-Ar	wr	16.1 ± 0.7	Gray and Miller, 1984a	32.0750	–112.7667	NAD27
3	2118	K-Ar	wr	16.7 ± 0.8	Gray and Miller, 1984a	32.0792	–112.9667	NAD27
Montezumas Head rhyolite (unit Nmr)								
		K-Ar	bio	17.5–16.0	Tosdal, et al., 1986			
4	UAKA-72-42	K-Ar	wr	17.4 ± 0.5	Shafiqullah et al., 1980	32.0672	–112.7088	NAD27
Childs Latite (units Nc)								
		K-Ar		18	Skinner, 2008			
Rhyolite of Pinkley Peak (units Np)								
5	AK2091	K-Ar	san	18.7 ± 0.5	Gray and Miller, 1984a	32.1181	–112.9667	NAD27
		K-Ar	bio	22–18	Tosdal et al., 1986			
Schuchuli granite (unit P_Es)								
		K-Ar	bio	23	Tosdal et al., 1986			
Gunsight Hills granodiorite (unit Kg)								
		U-Pb	zir	≈ 67	Tosdal et al., 1990			
Senita Basin granite (unit Ks)								
6	SENB	U-Pb	zir	67.7 ± 1.8	Rossi et al. 2023	31.5186	–112.8613	WGS84
Aguajita Spring granite (unit Ka)								
7	JITA	U-Pb	zir	80 ± 3	Rossi 2022; Rossi et al., 2023	31.9441	–113.0112	WGS84
Pozo Nuevo granite porphyry (unit Japn)								
8	QB-J2	U-Pb	zir	168 ± 6	Rossi, 2022; Rossi et al. 2023	32.0017	–113.0549	WGS84
9	QB-J8	U-Pb	zir	178 ± 6	Rossi, 2022; Rossi et al. 2023	32.0058	–113.0578	WGS84
Metamorphosed quartz porphyry (unit Jaq)								
10	QB-1	U-Pb	zir	170 ± 4	Rossi, 2022; Rossi et al. 2023	31.9992	–113.0537	WGS84
Orthogneiss and foliated granite (unit Xo)								
11	QB-J4	U-Pb	zir	1639 ± 37	Rossi, 2022; Rossi et al. 2023	31.9981	–113.0526	WGS84

[1]NAD27, North American Datum of 1927; WGS84, World Geodetic System 1984.

as well as in southwest and west-central Arizona and adjacent southern California (e.g., Tosdal et al., 1989; Fackler-Adams et al., 1997; Anderson et al., 2005b; Tosdal and Wooden, 2015; Busby and Centeno-García, 2022). Specifically, unit Jaq of OPCMN, 170 ± 4 Ma (Rossi, 2022), is correlative (within the uncertainty of respective U-Pb ages) with the Ali Molina Formation, 170 ± 3 Ma, of the Topawa Group in the Baboquivari Mountains and the Pajarito tuff (of Riggs and Busby-Spera, 1991), 170 ± 5 Ma, in the San Luis and Las Guijas Mountains (Fig. 1; Riggs and Haxel, 1990; Riggs, et al., 1993; Haxel et al., 2005). The Ali Molina and Pajarito units are distinctive in that they include interbeds of quartz arenite (and derivative quartzite), in part aeolian. In contrast, the quartz porphyry of unit Jaq, much of which is extrusive, lacks quartz arenite or quartzite. The paleogeographic significance of this difference has yet to be explored.

The Jurassic magmatic arc developed in a setting of crustal extension (Busby-Spera, 1988; Busby and Centeno-García, 2022). In Late Jurassic time, extension was accompanied by a distinctive new assemblage of igneous rocks, in southern Arizona represented by the Ko Vaya Suite (Tosdal et al., 1989; Beikman et al., 1995; Haxel et al., 2008a). This synextensional suite is best developed or preserved in the region east of OPCNM, particularly the North and South Comobabi Mountains and adjacent ranges (Fig. 1). The Ko Vaya Suite is imprecisely dated, but U-Pb interpreted ages are ≈ 160–145 Ma, mostly in the younger part of this age range. We presume, provisionally, that similar (but undated) rocks in OPCMN—units Jr, Jh, Jhp, and Jg—likewise are Late Jurassic.

The final Jurassic episode was continued crustal extension and basin formation (Busby et al., 2005). Coarse conglomerate, unit Jc, is exposed in only a few places in the OPCNM region, notably near Scarface Mountain. This unit probably is broadly correlative with the latest Jurassic (to earliest Cretaceous?) Glance Conglomerate of southeast and south-central Arizona (e.g., Bilodeau, et al., 1987; Dickinson and Lawton, 2001; Bassett and Busby, 2005; Haxel et al., 2008a). Formation of basins in which Glance Conglomerate accumulated may have been related to a major strike-slip fault, the Sonora-(Mojave?) megashear, in northern Sonora (Anderson et al., 2005b; Anderson and Nourse, 2005).

Late Cretaceous to Early Neogene ("Laramide"): Granitoid Plutonism, Thrust Faulting, and Regional Metamorphism

Subduction-related magmatism in southern Arizona and northwest Sonora resumed in Late Cretaceous or early "Laramide" time (Greig and Barton, 2019). The oldest Late Cretaceous granite in the OPCNM region is the ≈ 80 Ma Aquajita Spring pluton. Late Cretaceous granitoids this old are uncommon in southern Arizona. The Aquajita Spring granite is best regarded as not an aspect of the Arizona Laramide episode but rather an eastern satellite of the Peninsular Ranges batholith of Baja and southern California. (The Peninsular Ranges batholith was considerably closer to OPCNM before late Cenozoic opening of the Gulf of California: Bennett and Oskin, 2014; Umhoefer et al., 2018). Moreover, the Aquajita Spring granite is allochthonous, having been transported northward on the Quitobaquito thrust (see below).

The main phase of Laramide magmatism, which produced numerous porphyry Cu deposits (Barton et al., 1995; Lang and Titley, 1998; Staude and Barton, 2001; Greig and Barton, 2019; Haxel et al., 2022), is represented in the OPCNM region by the Bandeja Well and Gunsight granodiorites (units Kb, Kg; both ≈ 67–68 Ma) within and north of the map area, as well as the Cornelia granodiorite (age between 72 and 65 Ma: Cox et al., 2006) exposed near Ajo, ≈ 15 km north of the Monument boundary. These three granitoids, along with the genetically related volcanic rocks of unit Kv (72 Ma), are representative of Late Cretaceous calcalkaline, metaluminous, intermediate-composition magmatism in southern Arizona.

The map includes one more Late Cretaceous granitoid unit, the Senita Basin granite (unit Ks), U-Pb zircon age 68 Ma (Rossi et al., 2023). The Senita Basin granite is coeval with and lithologically similar to the Gunnery Range batholith, extensive in the region west to Yuma and southwest into northwest Sonora (Richard et al., 2000; J.V. Chapman, University of Texas El Paso, written communication, 2022).

In Late Cretaceous through early Paleogene time, the crust of southern Arizona and north Sonora was reworked by the Laramide orogeny. In south-central Arizona, this orogenic event involved thrust faulting, regional metamorphism, and melting of the lower crust to produce peraluminous leucogranites (e.g., Haxel et al., 1984; Nourse et al., 1994; Chapman et al., 2021, 2023). One of these thrust faults is the mylonitic Quitobaquito thrust (Fig. 6), well exposed along a length of 5 km in the eponymous range. Unlike other Laramide thrust faults in southwest Arizona, which have single lower plates, the Quitobaquito roof thrust is underlain by a duplex of some eight imbricate structural sheets, the La Abra complex, separated by mylonitic shear zones (Fig. 7). A single blastomylonitic to, locally, mylonitic or crystalloblastic metamorphic fabric, with consistently oriented foliation and lineation, extends continuously from the lower part of the upper plate of the Quitobaquito thrust down through the entire several-kilometer thickness of imbricate lower-plate sheets. This tectonite fabric is most strongly developed within the mylonitic zones bounding the sheets and decreases in intensity into the interiors of the sheets. Thus, contacts between sheets are synmetamorphic shear zones marked by intensification of the regional metamorphic fabric. Greenschist- to lower-amphibolite-facies metamorphism of the La Abra complex was consequent to tectonic burial beneath the Quitobaquito thrust.

The north-directed Quitobaquito thrust juxtaposes two unrelated terranes: the Jurassic La Abra complex below and Paleoproterozoic gneiss plus Late Cretaceous Aquajita Spring granite above (Haxel et al., 1984; Rossi, 2022; Rossi et al., 2023).

Both upper-plate units have Sonoran affinities. The orthogneiss belongs to the Caborca block (Iriondo et al., 2005), an evidently out-of-place crustal domain in northwest Sonora (Anderson et al., 2005a). As already mentioned, the Aquajita Spring granite is probably related to the eastern margin of the Peninsular Ranges batholith. Displacement on the Quitobaquito fault is unknown but likely substantial, possibly tens of kilometers.

Elsewhere in southwest Arizona, Laramide regional metamorphism was accompanied by intrusion of late-kinematic peraluminous leucogranites, typically ≈ 58 Ma (e.g., Wright and Haxel, 1982; Haxel et al., 2022; Chapman et al., 2023). Outcrops nearest OPCNM are in Sierra Blanca and the Kupk Hills (Fig. 1). In the original synthesis by Haxel et al. (1984), the Senita Basin granite was considered one of these leucogranites. Subsequently geochronologic, regional, and geochemical data indicate the Senita Basin granite does not belong to this late-kinematic suite.

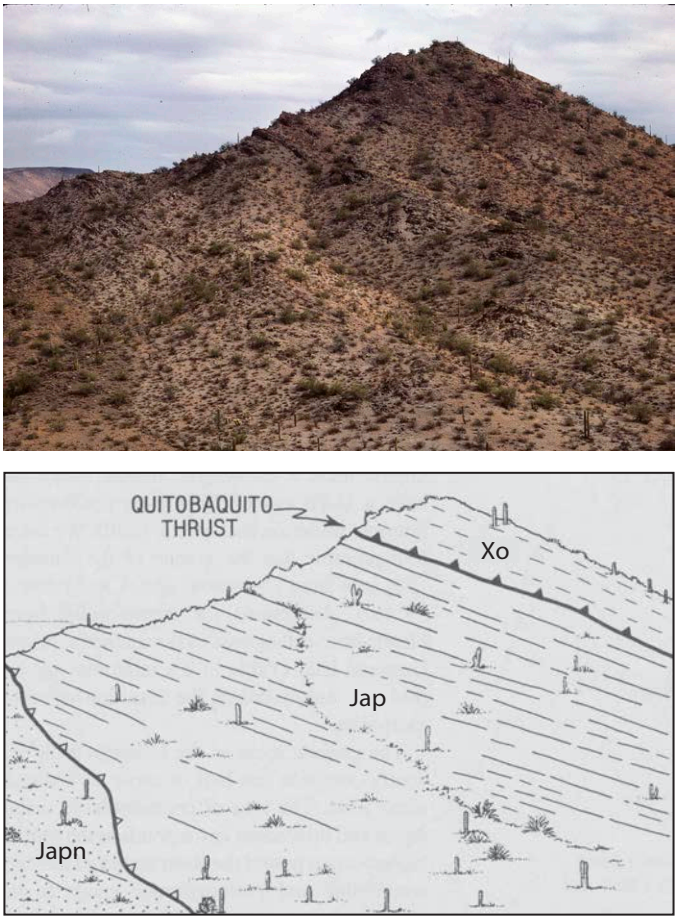


Figure 6. Gently south-southeast–dipping Quitobaquito thrust, north-central Quitobaquito Hills. Lithologic units: Xo, Paleoproterozoic orthogneiss; Jap, quartzofeldspathic semischist and phyllite; Japn, Pozo Nuevo granite porphyry (Fig. 18). The latter two are Middle Jurassic, metamorphosed in latest Cretaceous to early Paleogene time. They are separated by a minor, subsidiary shear zone (open barbs). Hill ≈ 50 m high. Sketch after Haxel et al. (1984). Photographs (except Figure 11D) by the authors.

Late Oligocene to Late Miocene: Volcanism and Crustal Extension

The dramatic topography of OPCNM, characterized by jagged mountain peaks poking out of broad alluvial plains, was largely shaped by the last major tectonic episode in the desert Southwest: late Oligocene to Miocene Basin and Range volcanism and crustal extension.

Volcanic rocks in OPCNM make up the southwest part of the Ajo volcanic field (Fig. 8), which covers an area of some 5,000 km² surrounding that town. The Ajo volcanic field is a thick, compositionally diverse volcanic sequence (Figs. 3, 5) unconformably overlying Paleoproterozoic through early Paleogene crystalline rocks. Volcanism spans a depositional period of approximately 8 million years (Table 1), beginning ≈ 22 Ma with silicic to intermediate dome intrusions, effusive lava flows, and explosive eruptions and ending ≈ 14 Ma with mafic flows, flow breccias, and explosive vents. The Ajo volcanic rocks were first described and named by Gilluly (1946). Complete volcanic stratigraphy was delineated by May et al. (1981) and later expanded to include rocks in 12 regional mountain ranges by Gray and Miller (1984a; 1984b), Gray et al. (1985), Tosdal et al. (1986), and Gray et al. (1988). Volcanic and coeval plutonic rocks are divided into four groups deposited in rapid succession separated by short erosional interludes: Pinkley Peak rhyolite (units Np), Childs Latite and coeval plutonic rocks (units Nc), Montezuma Head rhyolite (units Nm), and Batamote Andesite complex (units Nb).

The base of the Neogene OPCNM volcanic sequence is the Pinkley Peak rhyolite (22–18 Ma); silicic lava flows, tuffs, and associated volcaniclastic rocks. Within the Monument these rocks are limited to the northern Puerto Blanco Mountains, Cypriano Hills, and Bates Mountains. Childs Latite volcanic and coeval plutonic rocks (18 Ma), which comprises much of the Ajo volcanic field within the Monument, unconformably overlies Pinkley Peak rhyolite or intrudes other older rocks, and are characterized by distinctive megacrystic plagioclase porphyry. Montezuma Head rhyolite flows, flow breccias, and minor volcaniclastic rocks (17–16 Ma) cap Childs Latite and are exposed only within the Ajo Range. The youngest volcanic sequence within OPCNM, the Batamote Andesite complex, is a mafic to intermediate sequence of basalt, basaltic andesite, and minor dacite (16–14 Ma). Those rocks unconformably overly Childs Latite, Montezuma Head rhyolite, and/or Daniels Conglomerate (unit Ndc) and are exposed throughout much of OPCNM in the Growler Mountains, Bates Mountains, and southern Ajo Range.

Volcanism in OPCNM was synchronous with extension through at least middle Miocene time (Spencer et al., 1995). A thick sequence of coarse clastic sedimentary rocks exposed in the Little Ajo Mountains north of the Monument boundary and north of this map extent, in particular the eastward-thickening Locomotive Conglomerate (Spencer et al., 1995), records a minimum age of extension in the OPCNM region around



Figure 7. Steeply dipping tectonic sheets (Haxel et al., 1984, Fig. 7), northern Puerto Blanco Mountains; views eastward. **(A)** Two sheets of metamorphosed Pozo Nuevo granite porphyry (unit Japn; Fig. 18), center and left, are separated by steeply north-dipping mylonitic shear zone, in the valley left of center. To right is metamorphosed quartz porphyry (unit Jaq; slightly lighter colored; Fig. 17), separated from the central Japn sheet by another mylonite zone (image B). **(B)** Closeup of part of right side of image A. Mylonitic shear zone, marked by prominent planar foliation, between metamorphosed Pozo Nuevo granite porphyry (unit Japn, reddish weathering) on left and metamorphosed quartz porphyry (unit Jaq, light gray) on right. A, Ajo Range on skyline; B, Pinkley Peak on right skyline.

23 Ma (Gray and Miller, 1984a). Within OPCNM, younger, thinner packages of Miocene sedimentary rocks interbedded with Childs Latite and Batamote Andesite complex rocks record continued extension into middle Miocene time: Daniels Conglomerate exposed in Growler Mountains and Ajo Range (unit Ndc) and Neogene sedimentary rocks exposed in the northern Ajo Range (Nsv).

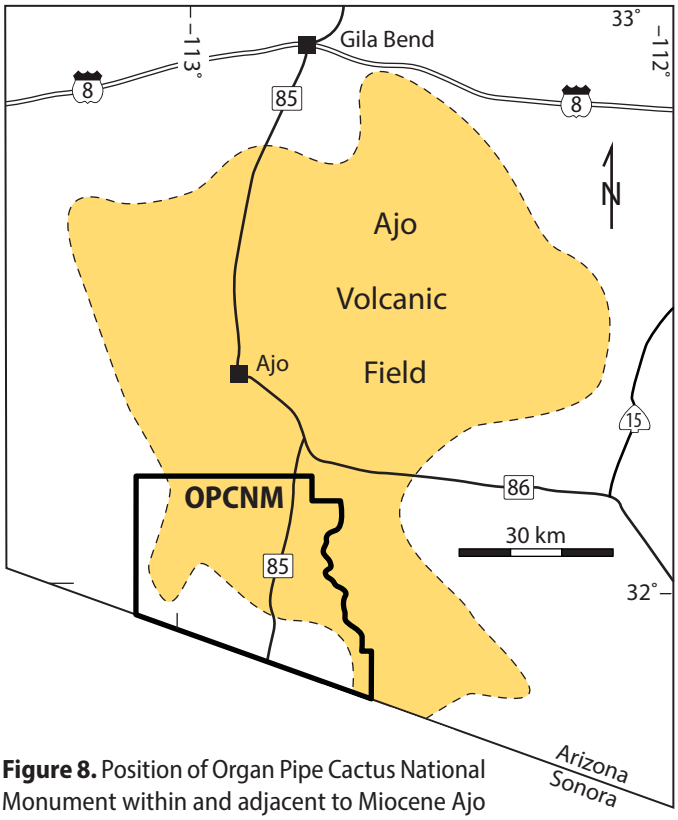


Figure 8. Position of Organ Pipe Cactus National Monument within and adjacent to Miocene Ajo volcanic field, southwest Arizona (Spencer et al.,1995; Richard et al., 2000).

Extension within OPCNM was relatively minor compared to most other areas of the Arizona and Sonora Basin and Range. Older volcanic rocks, of the Pinkley Peak, Childs, and Montezuma Head units (Fig. 5), mostly dip ≤ 20°, but locally as much as 35° near north-northwest–striking high-angle normal faults. Most of these faults have no more than several hundred meters of separation. No low-angle extensional ("detachment") faults are exposed within the Monument. Rocks of the youngest volcanic unit, the Batamote Andesite complex, unconformably overly older rocks, indicating the episode(s) of gentle tilting that affected the three older volcanic units had waned by Batamote time. Though Batamote rocks are cut by a few normal faults, gentle dips within this unit are generally depositional.

Pliocene to Present: Aggradation and Incision

Surficial deposits covering broad alluvial plains in the Valley of the Ajo, Sonoyta Valley, La Abra Plain, the upper drainages of Growler and San Cristobal Washes, and numerous smaller valleys (Fig. 2) comprise mainly alluvial gravel and sand, fining away from margins of ranges. In the original field mapping, all Quaternary deposits were included in a single unit. On the present map we distinguish one surficial unit (Qg): alluvial-fan gravel flanking the northern Ajo Range and Cipriano Hills (unit Qg). Other Quaternary deposits are unmapped. Surficial deposits in the eastern part of OPCMN are mapped in detail by Pearthree et al. (2020), Youberg and Pearthree (2020), and Young and Pearthree (2020).

DESCRIPTION OF MAP UNITS

Previously defined formal geologic names (Gilluly, 1946; Haxel et al., 2005, 2008a; others) are indicated by uppercase lithologic terms, for example *Batamote Andesite*. Informal geologic units

introduced for this report are indicated by lowercase lithologic terms, as in *Montezuma Head rhyolite*.

Asterisks (e.g., **Npb** Olivine-augite basalt dikes *) indicate map units for which no detailed lithologic description is available.

Quaternary Surficial Deposits

Qg Alluvial-fan gravel

Alluvial-fan gravel unconformably overlying Pinkley Peak rhyolite (units Np), Montezuma Head rhyolite (units Nm), and Batamote Andesite complex rocks (units Nb), in the northern Ajo Range and Cipriano Hills. Also present but not mapped in other areas.

Neogene and Late Paleogene Rocks, Largely Volcanic

Neogene and late Paleogene volcanic and minor sedimentary rocks of OPCNM (Fig. 5) include four major groups (youngest to oldest): Batamote Andesite complex, Montezuma Head rhyolite, Childs Latite, and Pinkley Peak rhyolite. These groups are described first. Eight less-extensive units are then described in subsection "Miscellaneous Igneous and Sedimentary Rocks" (p. 15): Nd, Nh, Nr, Ndc, Nt, Nv, Nsv, and P_Es.

- **Batamote Andesite complex (middle Miocene; units Nb)**

Gray to black or red-brown (oxidized) basalt, basaltic andesite, and andesite flows, flow breccia, agglomerate, and dikes. Flows cap mesas in Growler Mountains, Bates Mountains (Fig. 9), Cipriano Hills, and southern Ajo Range. Includes minor interbedded lenses of pyroclastic rocks, paleosol horizons, and volcaniclastic(?) sandstone and conglomerate. K-Ar ages are ≈ 16–14 Ma (Table 1). Type area is the Batamote Mountains, northeast of Ajo (Gilluly, 1946; Bowles and Greeley, 2013).

Nbb Porphyritic basalt

Medium-gray to black porphyritic basalt, as flows ≈ 100 m thick. This unit, limited in extent, occupies the same stratigraphic position as basaltic andesite flows (unit Nba). Basalt overlies Daniels Conglomerate (Ndc) and rhyolite (Nr) and crops out only on several plateaus in the southern Growler Mountains near Growler Pass. Composed of 60 percent or more phenocrysts of subhedral and anhedral iddingsite-rimmed olivine; lath-shaped twinned plagioclase (0.3–1 mm) showing faint oscillatory zoning; and zoned clinopyroxene commonly in glomeroporphyritic clusters with plagioclase and altered olivine. Groundmass is interstitial to hyalopilitic, comprising randomly oriented plagioclase, granular clinopyroxene, magnetite, brown glass, rare olivine, and secondary calcite.



Figure 9. Batamote Andesite complex (units Nb), Bates Mountains. Kino Peak near center.

Nba Basaltic andesite flows and flow breccias

Porphyritic, medium-gray to black basaltic andesite with reddish, oxidized flow margins. Maximum thickness is ≈ 300 m. Individual flows are 2–10 m thick and commonly separated by oxidized basal flow breccia and vesicular, glassy upper margin; minor lenses of pyroclastic rocks occur between flows and at the basal contact of the unit; thick paleosol horizons separate some flows. Multiple flow sequences are best exposed near Temporal Pass (north of the Monument boundary). Except for slight modal variation in phenocryst content, flows are uniform bottom to top. Unit dips gently (7–14°) eastward. Unit base generally rests upon an irregular surface of Daniels Conglomerate (unit Ndc), and locally on monzonite, rhyolite, or rhyolite breccia (Nr).

Phenocrysts, 5–15 percent of rock, comprise subhedral olivine (0.5–2.5 mm), partially or completely altered to iddingsite (prominent in hand specimen), minor euhedral to subhedral plagioclase, twinned clinopyroxene, and rare orthopyroxene. Glomeroporphyritic texture is common. Pilotaxitic to intergranular groundmass comprises plagioclase feldspar, clinopyroxene, magnetite, and slightly devitrified brown glass.

Basaltic andesite is the youngest volcanic unit within OPCNM and forms minor dikes observed intruding all other units. Whole-rock K-Ar ages for samples collected at or near the exposed top of this unit are 14.4 ± 0.7 Ma and 15.0 ± 2.2 Ma (Table 1).

Nbai Vent intrusive rocks

Volcanic plugs and dikes. Plugs are dark-colored fine- to medium-grained intergranular to pilotaxitic basalt; composed of partly resorbed iddingsite-rimmed olivine phenocrysts (1–2 mm) set in an intergranular matrix of plagioclase, clinopyroxene, magnetite, minor glass, and secondary calcite. Olivine phenocrysts are less altered in intrusive rock than in related flow units.



Figure 10. Montezuma Head rhyolite (units Nm), Ajo Range; showing typical steep, rugged topography. **(A)** Arch Canyon. Yellow flowers are brittlebush (*Encelia farinosa*). **(B)** Cacti in foreground: organpipe (multistemmed) and saguaro (columnar) .

Nbab Vent breccias

Reddish-brown to brown, crudely bedded pyroclastic rocks, thickness to ≈ 130 m, consisting almost entirely of subrounded to angular scoriaceous ejecta (1 mm to 3 cm); fragments are moderately sorted; rock is locally zeolitized and partially cemented by caliche. Dikes of basaltic andesite intrude the breccia. Breccias dip steeply away from central vent areas, are crosscut by vent intrusive rocks, and are overlain at vent borders by massive nearly horizontal flows.

Nbu Flows, flow breccias, and vent intrusive rocks, undivided

- **Montezuma Head rhyolite (early Miocene, units Nm)**

Thick, stubby rhyolite flows, plugs, and associated tuff and tuff breccia. Unit includes minor dacite and andesite flows, and volcaniclastic sedimentary rocks. Within OPCNM, Montezuma Head rhyolite comprises much of the central Ajo Range (Fig. 10). Except for porphyritic basalt (unit Nmb), volcanic units have several petrographic characteristics in common: (1) subhedral to euhedral, moderately to strongly embayed, sieve-textured plagioclase phenocrysts; (2) phenocrysts(?) of augite, biotite (commonly replaced by magnetite), oxyhornblende (commonly opaque-altered), and hypersthene; (3) black to gray crystallite-rich groundmass consisting of perlitic glass, and fine-grained quartz, feldspar, magnetite, limonite, and unidentified clay minerals. K-Ar ages are biotite 17.5–16.0 Ma, whole-rock 17.4 ± 0.5 Ma (Table 1).

Nma Augite andesite and hypersthene-hornblende andesite of Ajo Range

Red-brown, gray, black, or purple augite andesite flows, lahars, tuff breccias, agglomerate, and minor black hypersthene-hornblende andesite flows. Unconformably overlies Childs Latite (unit Ncl) or is interbedded with rhyolite (Nmr). Likely contemporaneous with dacite flows (Nmd). Augite andesite flows are locally layered; reddish-brown partially oxidized. Andesite lava is succeeded upward by dense, black andesite vitrophyre and gray, platy andesite. Individual flow layers are aphyric or contain phenocrysts or microphenocrysts of subhedral to fragmental augite and weakly zoned plagioclase in a hyalopilitic groundmass of moderately oriented plagioclase microlites, sparse clinopyroxene, magnetite, and glass.

Hypersthene hornblende andesite flows are porphyritic. Phenocrysts are subhedral to euhedral of hypersthene, hornblende, and plagioclase; in a brown glassy matrix.

Nmu Montezuma Head rhyolite, undivided

Nmat Crystal-lithic ash-flow tuff

Brown to orange, poorly to densely welded tuff containing angular basalt and andesite lithic fragments (mostly < 3 cm, locally as much as 15 cm), ≈ 70 m thick. Vapor-phase recrystallization and devitrification are variable. Unconformably overlies varyingly zeolitized tuff (unit Nmt) near Tillotson Peak, underlies Batamote Andesite (Nba) in Bates Mountains. Forms prominent resistant cliffs in Diablo Mountains.

Nmr Rhyolite and minor dacite flows, flow breccias, and plugs

Rhyolite and dacite; fresh surfaces are red, purple, brown, gray, or black. Weathered surfaces are tan, brown, or maroon and partially stained with Mn oxides. Rhyolite flows are short and stubby, locally overlie white to yellow tuff breccia (unit Nmt), and can be traced to vent sources.

Aphyric to moderately porphyritic dacite flows are sheet-like with locally zeolitized flow margins. Flow banding occurs on all scales and is commonly contorted; groundmass exhibits microscopic fluxion banding. Subhedral to euhedral and

commonly fragmental phenocrysts include plagioclase and biotite, less common augite, diopsidic augite, oxyhornblende, sanidine, and bipyramidal quartz. Biotite is partially oxidized and locally rimmed by augite and quartz. Most oxyhornblende is altered to magnetite. Groundmass is vitrophyric to hyalopilitic.

In glassy rocks, matrix comprises black or gray perlitic glass-bearing lath-shaped crystallites and tan to brown spherulites. Where strongly recrystallized or felsitic, the groundmass consists of interlocking quartz, alkali feldspar, and magnetite (commonly altered to brown limonite). Limonite-rimmed quartz fills voids where vapor-phase crystallization is pervasive. Unit locally includes unmapped horizons of tuff and tuff breccia (Nmt) and dikes. Forms massive, nearly vertical cliffs, steep slopes, flat benches, and ledges throughout the Ajo Range (Fig. 10).

Nmt Tuff and tuff breccia

Buff, yellow, greenish, and white crystal-vitric and lithic-lapilli tuff, tuff-breccia, agglomerate, and tuffaceous sandstone; ≈ 100 m thick. Massive or stratified with well-developed internal stratification and cross-bedded; individual beds range from < 5 cm to 5 m thick. Forms continuous horizons or lenses within rhyolite flows (unit Nmr) and some beds are complexly contorted or folded by younger or contemporaneous rhyolite flows. Composed of fragmented phenocrysts and angular lithic fragments (Nmr) in a matrix of pumice lapilli and glass shards. Phenocrysts of strongly embayed plagioclase and quartz are common. Feldspar has bleb-like inclusions of diopsidic augite, augite, brown glass, and apatite prisms. Pumice fragments and shards are partly devitrified or varyingly recrystallized to quartz, alkali feldspar, iron oxides, or ubiquitous brown clay minerals. Diagenetic zeolitic alteration is common.

Nmb Porphyritic basalt of Diablo Mountains

Fine-grained, holocrystalline, weakly porphyritic basalt flow, intercalated with tuff (unit Nmt), weathers red, ≈ 15 m thick. Phenocrysts include olivine altered to iddingsite and plagioclase, normally zoned from labradorite to andesine, in a pilotaxitic groundmass of plagioclase microlites, clinopyroxene, olivine, and Fe-Ti oxides.

Nmd Dacite of Ajo Range

Brown, gray, and black porphyritic dacite flows interbedded with rhyolite (Nmr); locally includes sparse yellow tuff-breccia (unit Nmt). Phenocrysts are subhedral to euhedral or fragmental plagioclase; augite; and sparse hypersthene, hornblende, and biotite. Mafic phenocryst mineralogy varies among flows. Brown clay minerals are locally pervasive and commonly surround oxidized mafic phenocrysts. Groundmass is flow-banded crystallite. Although generally fissile and friable, exposures locally form distinct prominences, including reddish-brown ledges and cliffs in the Ajo Range.

- **Childs Latite and coeval plutonic rocks (early Miocene, units Nc)**

Volcanic rock sequence that includes augite latite, augite andesite, olivine augite basalt, and alkali basalt with coeval intrusive monzogranite and minor monzonite, erupted or intruded over a geologically short interval ≈ 18 Ma (Table 1). In OPCNM, Childs Latite is exposed in Ajo Range, northeastern Puerto Blanco Mountains, and Bates Mountains (Figs. 2, 11). Gilluly (1946) originally mapped, described, and named these rocks near Ajo. Further mapping has extended the known unit distribution to 12 mountain ranges in the surrounding area (Jones, 1974; Eberly and Stanley, 1978; May et al., 1981; Gray et al., 1985; Peterson et al., geologic mapping, 1979–1982; Bezy et al. 2000, p. 24–25).

Ncu Childs Latite and coeval plutonic rocks, undivided

Ncl Latite flows and flow breccias

Augite latite to trachyandesite with less abundant shoshonite and andesite flows, flow breccia, flow agglomerate, dikes, minor hypabyssal, and more silicic tuffaceous rocks characterized by megacrystic plagioclase phenocrysts (Fig. 11). Unit is ≈ 250–600 m thick; individual flows typically 5–10 m thick. Fresh surfaces are gray to black, or maroon and iron-oxide stained; weathered surfaces are tan, brown, or purple. Individual flows are evenly bedded, vesicular to massive, and generally lack internal flow features. Older flows are thicker, more massive, blue to gray, and less weathered, whereas younger flows are thinner, oxidized, and red to brown. Each flow typically has a basal flow breccia 1–3 m thick and a scoriaceous, oxidized upper flow surface. Interbedded with andesite and basalt (unit Nca) or Daniels Conglomerate (Ndc).

Flows have a porphyro-aphanitic to intergranular texture, ranging from holocrystalline to hyalocrystalline. Phenocrysts include plagioclase, euhedral to subhedral augite (less commonly diopsidic augite; < 1 mm long), biotite, oxyhornblende, locally abundant olivine with iddingsite rims, and sparse ilmenite, leucoxene, apatite, and zircon(?). Plagioclase (andesine to oligoclase-sanidine) megacrysts, 0.5–4 cm long, are euhedral, complexly oscillatory zoned and comprise 10–40 percent of the rock; margins are commonly embayed; cores contain abundant inclusions of apatite, augite, and devitrified brown glass.

Plagioclase size, abundance, and shape account for variation within and among separate flows. Groundmass is pilotaxitic, cryptocrystalline, or glassy and composed of plagioclase microlites, clinopyroxene, rare orthopyroxene, magnetite, glass, quartz, and olivine. Locally contains volcanic or granitic xenoliths.



Figure 11. Childs Latite (unit Ncl). **(A)** Lavas flows; Diaz Spire, southern Ajo Range. **(B)** Lavas flows; near Twin Peaks, eastern Puerto Blanco Mountains. **(C)** Megacrystic plagioclase phenocrysts; outcrop, Ajo Range. Knife 9 cm. After Bezy et al. (2000). **(D)** Plagioclase phenocrysts. Image courtesy of K. KellerLynn, NPS, 2023.

Nca Augite andesite

Augite andesite flows and flow breccia interbedded with Childs Latite flows (Ncl). Laterally discontinuous, ≈ 80 m thick, with individual flows 5–15 m thick. Unit is lighter colored and notably less porphyritic than surrounding Childs Latite flows. Fresh surfaces are weathered gray to tan, brown, gray, and maroon. Flows are massive and display local weak flow-banding, vesiculated tops, and brecciated bases, with minor auto-brecciated and scoriaceous flows. Flow sequences rest on a thin (< 2 m thick) poorly sorted, pebble- to cobble-size conglomerate composed exclusively of Childs Latite (Ncl) clasts. Flows are porphyro-aphanitic with < 2 cm–long phenocrysts comprising 15 percent of rock. Most abundant phenocrysts are euhedral laths of zoned labradorite and subhedral to euhedral, usually glomeroporphyritic, augite. Minor phenocryst constituents are oxyhornblende and biotite (oxidized to magnetite and hematite); euhedral apatite is an accessory phase. Pilotaxitic groundmass consists of plagioclase microlites, clinopyroxene, magnetite, hematite, and interstitial cryptofelsite. Vesicles and microveinlets are lined or filled with calcite or cristobalite and tridymite.

Ncb Olivine-augite basalt and alkali basalt

Brown, gray, and black olivine augite basalt, augite basalt, and alkali olivine basalt flows, flow breccias, and less common plugs and dikes, ≈ 100 m thick. Weathered surfaces are darker and black-brown, tan, and gray mottled. In southern Ajo Range, individual flows are 5–20 m thick (unit < 100 m thick); farther north, individual flows are < 2 m thick (unit < 10 m thick); dikes < 3 m thick. Flows are dense, massive to flow-banded, porphyritic, and vesicular; usually lenticular in cross section and laterally discontinuous. Flows commonly have red-brown, scoriaceous basal agglomerate, and flow tops bear flattened vesicles. Phenocrysts (5–15 %) include euhedral to subhedral, partially to completely iddingsitized olivine (0.5–1 mm); green, euhedral to subhedral, twinned augite (< 2 mm); and less common moderately zoned, locally glomeroporphyritic labradorite (< 4 mm). Rare accessory minerals are hypersthene, magnetite, and apatite. Groundmass is pilotaxitic and composed of plagioclase microlites and laths; intergranular clinopyroxene; olivine (commonly iddingsitized); secondary chlorite; magnetite; minor brown, partially devitrified glass; and minor calcite in veinlets and vesicles.

Ncm Monzogranite of Siovi Shuatak Wash and related rocks

Heterogeneous mix of monzogranite, monzogranite porphyry, and minor monzonite porphyry in the Ajo Range, first described by May et al. (1981). Fresh surfaces are gray, pink, purple, or red; weathered surfaces are mottled shades of gray, green, brown, white, tan, and orange.

Intrusive contacts with Childs Latite (unit Ncl) are complex and intergradational, suggesting the two units are coeval. Extremely variable textures include microcrystalline or cryptocrystalline and porphyritic to granitic. Intrusive breccias and thin, interfingering dikes are common. Phenocrysts, ≈ 1 cm long, are euhedral andesine, rimmed by alkali feldspar. Groundmass is fine- to medium-grained and composed of subhedral plagioclase, anhedral orthoclase, augite, biotite, hornblende, interstitial quartz, and disseminated magnetite. Accessory minerals are titanite and apatite. Argillic alteration and silicification are locally pervasive. Plagioclase is altered to sericite and clay minerals. Mafic minerals are altered to magnetite, chlorite, epidote, and calcite.

Ncd Augite latite dikes *

• Pinkley Peak rhyolite (early Miocene, units Np)

Silicic volcanic and sedimentary rock sequence that includes rhyolite, rhyodacite, and dacite flows, domes, and tuffs, as well as minor andesite and basalt flows with interbedded sandstone and conglomerate. Pinkley Peak rhyolite was first described as the basal unit of the Ajo volcanic field in the Gunsight Hills and northernmost Ajo Range (Tosdal et al., 1986). Later the unit was extended to include rocks of similar lithology and stratigraphic position in the northern Puerto Blanco Mountains, Cipriano Hills, and central Bates Mountains. K-Ar ages are ≈ 22–18 Ma (Table 1). Petrographic characteristics include: (1) Phenocrysts of plagioclase (commonly sieve textured with inclusions of partly devitrified glass and apatite), biotite, oxyhornblende, hypersthene, augite, and rare quartz and sanidine. (2) Groundmass comprising flow-banded glass, partly recrystallized to microcrystalline quartz, feldspar, magnetite, and clay minerals.

Npb Olivine-augite basalt dikes *

Npr Biotite rhyolite domes, flows, agglomerates, and tuffs

Gray domes characterized by massive interior and contorted flow banding along margins. Short, thick, stubby flows differ considerably in thickness, lateral extent, texture, and phenocryst content. Commonly porphyritic with phenocrysts of subhedral red-brown biotite, euhedral sanidine, solitary or glomeroporphyritic plagioclase (commonly enclosing euhedral apatite or titanite), and quartz. Groundmass comprises devitrified glass and spherulites. Agglomerate is composed of monolithologic angular to subangular cognate clasts in a gray, tuffaceous matrix, is poorly sorted, and forms a carapace along flow and dome margins. Associated tuffs are lenticular and discontinuous. K-Ar sanidine age is 18.7 ± 0.5 Ma (Table 1).

Nprd Rhyolite, rhyodacite, and dacite flows and flow breccias

Gray, black, or brown, typically flow-banded to intergranular. Includes minor lithic lapilli tuffs (unit Npt) and sheared rocks with pervasive fault gouge. Minor phenocrysts commonly form either of two mineral assemblages: (1) euhedral augite, hypersthene, biotite, glomeroporphyritic plagioclase and hornblende(?) or (2) fragmental to glomeroporphyritic plagioclase, biotite, rare quartz, sanidine, and hornblende(?). Plagioclase is zoned with partially resorbed cores. Groundmass is hyalopilitic. Recrystallized groundmass contains spherulites and perlitic cracks are abundant.

Npt Lithic lapilli tuff

White to yellowish-green, poorly sorted massive to well-bedded, commonly cross-bedded, lithic lapilli tuff. Individual beds are 1 cm to 1m thick. Composed of fragmental plagioclase and biotite phenocrysts, subrounded lithic fragments of augite andesite (unit Npa) and pumice lapilli (< 1 cm long) in a vitroclastic matrix. Matrix and lapilli composed of devitrified to brown clay minerals, yellowish-green celadonite(?), and zeolite(?) minerals. Interbedded with rhyolite, rhyodacite, and dacite flows (Nprd) and hornblende dacite (Nphd).

Nphd Hornblende dacite flows and agglomerate

Red-brown and gray hornblende dacite flows, and agglomerate comprising gray clasts of hornblende dacite in fine-grained, red-brown, tuffaceous matrix. Phenocrysts include subhedral to euhedral oxyhornblende, zoned plagioclase (andesine to oligoclase, commonly bearing apatite prisms), and hypersthene(?). Groundmass is hyalopilitic with abundant magnetite. Petrographically similar agglomerate contains phenocrysts of euhedral oxyhornblende, less abundant subhedral plagioclase, and hypersthene(?) in a hyalopilitic groundmass of plagioclase microlites, dusty Fe-Ti oxides, and glass.

Nps Arkosic and volcaniclastic sandstone

Beige, tan, and red-brown, well-bedded, moderately indurated arkosic and volcaniclastic sandstone and pebble conglomerate. Unit is interbedded with hornblende dacite (Nphd) and augite andesite (Npa). Pebbles are subangular clasts of Gunsight Hills granodiorite (Kg) and less commonly andesite. Well bedded; individual strata are 0.1 to 0.5 m thick.

Npa Augite andesite

Maroon, red-brown, and gray augite andesite flows. Phenocrysts include glomeroporphyritic, euhedral plagioclase, subhedral augite, sparse biotite, and magnetite (subhedral crystals or rims on or replaces mafic phenocrysts). Pilotaxitic groundmass is composed of plagioclase microlites; augite; rare partially devitrified, brown volcanic glass; and magnetite.

• Miscellaneous Igneous and Sedimentary Rocks

Eight minor units, of several ages (Fig. 5), grouped here for convenience (p. 10).

Nd Dikes * (Neogene)

Several dikes intruding faults, in western Quitobaquito Hills.

Nh Hornblende dacite * (middle Miocene)

Crops out in isolated hill east of Bates Mountains.

Nr Rhyolite flows, dikes, and pyroclastic rocks (middle Miocene)

In southern Growler Mountains, unit is rhyolite flows, flow breccias, and dike rocks of variable composition. In Batamote Mountains, unit is composed of light-gray to tannish-gray, reddish-brown to buff-brown feldspar- and biotite-porphyritic flows and tuffs. Phenocrysts include sanidine, quartz, and minor biotite and hornblende. K-Ar biotite age is 19.5 Ma ± 0.6 Ma (Gray and Miller, 1984a).

Ndc Daniels Conglomerate and associated lacustrine rocks (early Miocene)

Tan, gray, or red, poorly indurated, shallow-dipping, pebbly to sandy conglomerate; subordinate sandstone; and pebbly sandstone, ≈ 180–240 m thick. Subangular to subrounded clasts (5–20 cm) are locally derived, and dominant clast compositions mimic local bedrock units. Clasts are Cardigan Gneiss (exposed northwest of Little Ajo Mountains; Fig. 1); Chico Shunie Granite (exposed west of Little Ajo Mountains and central Growler Mountains); Mesozoic granite; and minor hornblende andesite and Childs Latite (unit Ncl). Coarse- to medium-grained arkosic matrix is poorly sorted and friable. Bedding is poorly defined with exception of pebbly sandstone showing subhorizontal 30-cm-thick bedding. Lacustrine sedimentary rocks, < 5 m thick, are purple-pink to tan, fine-grained siltstone and mudstone with < 5 cm-thick gypsum beds and locally include thin tuff (at top of section) and welded tuff (at base of section). Formally named by Gilluly (1946). Basal portion of Daniels Conglomerate interfingers with underlying Childs Latite (unit Ncl).

Nt Growler Mountain welded tuff (early Miocene)

Light-pink to -tan densely welded rhyolite tuff with flattened pumice fragments (3–5 cm), ≈ 30–60 m thick. Contains crystals of euhedral sanidine and biotite in a glassy matrix. Vapor-phase minerals occur along vesicle walls. Unit unconformably rests on Childs Latite (Ncl) and commonly forms 6–9 m-thick layers at base of Daniels Conglomerate (unit Ndc).

Nv Pyroclastic rocks * (early Miocene)

Pyroclastic rocks of intermediate composition in southern Sonoyta Valley, along the southern boundary of OPCNM.

Nsv Sedimentary and volcanic rocks (early Miocene)

Complex mix of poorly stratified, semi-consolidated red conglomerate; breccia; brown, fluvial conglomerate; sandstone; and minor gray and yellow tuff. Conglomerate, 20–100m thick, is composed of moderately to poorly indurated, crudely bedded, poorly sorted debris flows and fluvial gravel. Pebble- to boulder-size clasts are angular to subround, and are derived from Miocene volcanic rocks including Childs Latite (unit Ncl) (dominant), basalt, andesite, and rhyolite. The matrix is brown, pebbly, moderately sorted, and ranges from tuffaceous mudstone to sandstone. Locally includes dikes and flows of Montezuma Head rhyolite (units Nmd, Nmr), which are not mapped separately. The unit unconformably overlies Childs Latite (unit Ncl), underlies and is locally interbedded with Batamote Andesite complex basalt flows (unit Nbab), and overlies and is locally interbedded with Montezuma Head rhyolite tuffs (unit Nmt) and flows (unit Nmr).

P_Es Schuchuli granite (late Oligocene)

Grayish- and pinkish-tan, fine-grained, leucocratic biotite granite porphyry, forming a stock and small dike swarm. Five magmatic phases mapped by Tosdal et al. (1986) are here combined into a single unit. Composed of phenocrysts of subhedral to euhedral albite, embayed quartz, subhedral cloudy orthoclase, and subhedral biotite in a groundmass of orthoclase and quartz. Granophyre and, locally, albite phenocrysts are rimmed by micrographic quartz and orthoclase. Micrographic quartz and orthoclase compose as much as 30 percent of the groundmass and increase in abundance toward the north where granite porphyry becomes micrographic porphyry. Euhedral titanite, apatite, and zircon are accessory minerals. Miarolitic cavities, < 0.25 cm in diameter, increase in abundance toward the north. Two biotite K-Ar dates are ≈ 23 Ma.

Latest Cretaceous to Early Paleogene Chagit Vo gneiss

Gneissic and mylonitic orthogneiss derived from several phases of Gunsight Hills granodiorite (unit Kg). Tosdal et al. (1986)

mapped five facies, two of which crop out in our map area: protomylonitic granodiorite gneiss (unit KP_Ecp), blastomylonitic granodiorite gneiss (unit KP_Ecb); leucocratic granite gneiss, blastomylonitic monzogranite gneiss, and granodiorite gneiss. Highest-grade orthogneiss has K-Ar hornblende age 59 Ma, providing a minimum age of deformation and approximating cessation of metamorphism (Haxel et al., 1984).

KP_Ecp Protomylonitic granodiorite gneiss

Varies from slightly deformed enclaves of granodiorite to penetratively deformed and recrystallized protomylonitic gneiss characterized by strong metamorphic overprint of relict igneous texture. In gneissic rocks, quartz and biotite are strongly recrystallized; plagioclase and microcline only weakly so. Foliation is defined by ribbon quartz, chlorite, white mica, and metamorphic biotite. Relict sagenitic biotite is kinked and surrounded by finer-grained biotite, white mica, epidote, and titanite(?). Relict igneous plagioclase is partially to largely replaced by white mica, epidote, and locally calcite. Relict igneous microcline is partially granulated and marginally recrystallized to orthoclase and albite(?). Outcrop colors are light to medium gray to green-gray.

KP_Ecb Blastomylonitic granodiorite gneiss

Medium-gray, medium-grained granodiorite gneiss and subordinate dark-greenish-gray diorite gneiss; light-gray, medium-grained biotite monzogranite gneiss; and pinkish-weathering aplite gneiss; all with blastomylonitic foliation. Elongate quartz lenses and aggregates of feldspar and mica define west-plunging lineation. Microcline blastocrysts are fragmented with granulated rims of orthoclase and albite(?). Relict plagioclase phenocrysts are variably recrystallized to white mica and clinozoisite or have granulated rims of quartz and albite(?). These blastophenocrysts form augen surrounded by subidioblastic green-brown to green biotite, white mica, clinozoisite, and quartz. In diorite gneiss, blastocrysts of hornblende are rimmed and veined by biotite.

Late Cretaceous Leucocratic Granites

Two unrelated units of different ages. The Senita Basin granite (unit Ks), 68 Ma, is approximately the same age as three other Late Cretaceous igneous units—Kg, Kb, and Kv—but compositionally different and probably not petrogenetically related to them. The Aquajita Spring granite (Ka) is distinctly older, ≈ 80 Ma. Table 2 and Figure 12 document the compositional contrast between the highly silicic, Senita Basin and Aquajita Spring leucogranites (units Ks, Ka), with SiO_2 mostly 71 percent and FeO* + MgO + CaO mostly < 5 percent; and the compositionally expanded, intermediate, metaluminous rocks of the Gunsight Hills and Bandeja Well granodiorites (units Kg, Kb) and similar plutons, with $SiO_2 \leq 67$ percent and FeO* + MgO + CaO mostly ≥ 7 mass percent.

Ks Senita Basin granite (latest Cretaceous)

Leucocratic, moderately peraluminous granite (Fig. 13; Table 2), comprising two mesoscopically distinct phases (Tosdal et al., 1990): (1) Older leucocratic biotite syenogranite in which muscovite and garnet are sparse or absent. This granite is medium- to coarse-grained; pink to reddish weathering; generally equigranular but locally porphyritic, with alkali feldspar megacrysts ≤ 1 cm; and in part foliated, some places strongly so. (2) Younger highly leucocratic muscovite-bearing alkali-feldspar granite, with or without biotite and/or garnet. This phase is fine-grained to pegmatitic, white weathering; and unfoliated to weakly foliated. The older phase makes up the central part of the Senita Basin stock; the younger phase is concentrated near the margins and as dikes intruding the country rocks. Much of the granite is cut by sparse to common veins of sericite or, less commonly, white quartz. Primary and supergene sulfide, carbonate, and chloride minerals in quartz and quartz-calcite veins in the eastern part of the stock and its country rocks were mined, in the late 1800s and early 1900s, for small quantities of Pb, Ag, Cu, Zn, and Au (Keith, 1974; KellerLynn, 2022). A Monument hiking trail leads to two of these old mines.

The Senita Basin stock displays two intrusive styles. On the north and northeast sides of the stock, the unit is unfoliated and its country rocks (unit Jaq) are hornfelsic, Fe-oxide stained, and locally contain quartz-sericite veins. On the southwest and southeast sides, the roof of the stock, the unit is foliated and surrounded by a synplutonic dynamothermal aureole of quartzofeldspathic schist (see unit Jaqm).

U-Pb zircon age of Senita Basin granite is 67.7 ± 1.8 Ma (Rossi et al., 2023). The granite may be related to the coeval and lithologically similar Gunnery Range batholith, extensive in the region from OPCMN west to Yuma and southwest far into northwest Sonora (Richard et al., 2000; T.H. Anderson, University of Pittsburg, oral communication, ca. 1982; Haxel, reconnaissance, 1997; J.V. Chapman, University of Texas El Paso, written communication, 2022).

A sample of the young phase of the Senita Basin granite is notable for its unusual composition (Table 2, OP168; Fig. 12). This highly evolved, high-silica, garnet- and muscovite-bearing leucogranite has low concentrations of three groups of normally incompatible trace elements: Sr, Ba, and Eu; light rare earth elements (e.g., La, Ce, Nd) and Th; and Zr. Pronounced depletion in these three groups of elements owes to prolonged fractionation of, respectively, feldspars, monazite, and zircon. Relatively high Mn correlates with presence of accessory Fe-Mn garnet. Niobium and Ta are strongly enriched. Interelement ratios Zr/Hf and Nb/Ta are abnormally low, typical of highly evolved leucogranites (Černý et al., 1985; Bau, 1996).

Table 2. Representative whole-rock analyses of Late Cretaceous plutonic rocks, Organ Pipe Cactus National Monument and vicinity, southwest Arizona

Unit	Gunsight Hills granodiorite		Bandeja Well granodiorite		Aquajita Spring granite		Senita Basin granite	
							Old phase	Young phase
Sample	GH7	GH24	OP237	PUP50	OP784A	OP687	OP157	OP168
Major-element oxides (mass percent)								
SiO_2	61.8	66.5	65.7	67.1	73.3	76.0	75.0	76.4
TiO_2	0.80	0.53	0.57	0.54	0.22	0.03	0.20	<0.02
Al_2O_3	17.1	15.8	16.4	15.9	14.0	13.3	13.1	13.6
Fe_2O_3	2.30	1.88	1.88	1.78	0.93	0.37	0.66	0.08
FeO	2.66	1.28	1.51	1.51	0.66	0.12	0.71	0.17
MnO	0.09	0.05	0.05	0.05	0.04	<0.02	<0.02	0.20
MgO	2.36	1.34	1.53	1.37	0.56	0.10	0.40	<0.10
CaO	4.64	3.35	3.44	3.18	1.59	0.90	0.52	0.18
Na_2O	4.03	3.93	4.18	4.02	3.39	3.50	3.32	4.54
K_2O	2.80	3.36	3.37	3.41	4.54	4.89	5.32	4.05
P_2O_5	0.28	0.18	0.18	0.18	0.08	<0.05	0.05	<0.05
H_2O	0.94	0.88	0.57	0.42	0.35	0.10	0.24	0.19
CO_2	0.02	0.43	0.20	0.01	0.01	<0.01	<0.01	<0.01
Σ	100.3	99.5	99.9	99.8	100.4	99.4	99.7	99.5
Trace elements (µg/g)								
Rb	96	85	77	101	105	213	120	400
Cs	4.95	4.52		2.13			5.93	2.81
Sr	850	600	640	650	280	150	86	<20
Ba	1100	1040	890	950	810	210	540	<20
Sc	8.14	5.54	<10	4.50	<10	<10	3.56	1.23
V	120	74	92	91	<10	<10	<10	<10
Cr	16.3	9.31	12.	7.96	<10	<10	0.40	0.33
Co	12.1	7.96	9.8	6.62	2.8	<1.0	1.64	0.137
Ni	17	10	13	12	4.4	2.0	1.5	<1
Cu	8.5	12	9.2	8.4	3.9	8.5	8.1	<1.0
Zn	75	52	50	51	<50	<50	<50	<50
Zr	148	117	130	132	107	51	135	33
Hf	3.83	3.46		3.77			4.21	3.25
Nb	11.0	11.0		8.8			12.0	65.
Ta	0.809	0.670		0.613			1.47	18.1
Mo	0.67	0.55		0.45			0.39	0.23
W	0.50	0.40		0.16			0.44	0.24
Ga	24	19	20	20	19	27	12	41
Sn	6.3	1.4		1.2			0.80	2.0
Pb	19	23	17	21	27	41	19	12
Sb	0.076	0.156		0.071			0.064	0.031
F	600	<100	500	500	400	<100	600	200
La	34.9	22.7	33	27.9	<20	<20	34.6	2.14
Ce	66.0	49.1		50.6			65.4	4.75
Nd	29.9	22.7		22.5			26.6	9.20
Sm	5.21	4.05		3.88			6.52	1.32
Eu	1.35	1.04		1.01			0.592	0.044
Gd	3.76	2.98		2.40			7.86	
Tb	0.495	0.369		0.373			1.48	0.319
Dy	2.66	1.94		1.84			9.60	2.00
Tm	0.21	0.17		0.142			<1.5	
Yb	1.26	0.938		0.828			7.13	1.33
Lu	0.220	0.135		0.126			1.01	0.209
Y	18	11	14	13	<10	<10	68	14
Th	7.47	6.93		7.06			25.8	3.40
U	2.64	5.29		3.02			6.64	5.01
Elemental ratios								
AlSI	0.95	0.98	0.98	0.99	1.05	1.05	1.08	1.12
Zr/Hf	39	34		35			32	10
Nb/Ta	14	16		14			8.2	3.6
$(La/Yb)_{cn}$	19	17		23			3.3	1.1
Eu/Eu*	0.92	0.90		1.00			0.25	0.08

For all samples S reported as ≤ 100 µg/g.

AlSI = alumina saturation index = Al_2O_3 /(CaO+Na_2O+K_2O), molar. AlSI <1.00, metaluminous; AlSI > 1.00, peraluminous.

Nominal Zr/Hf, Nb/Ta for global upper continental crust: 33–36, 12–13.

cn, chondrite-normalized (Pourmand et al., 2012).

Eu*, Eu interpolated (logarithmically) between Sm and Gd or Sm and Tb.

Analytical methods (Baedecker, 1987): Most major-element oxides: wavelength-dispersive x-ray fluorescence. Trace elements: energy-dispersive x-ray fluorescence, instrumental–neutron-activation analysis, spectrophotometry, quantitative emission spectroscopy.

Ka Aquajita Spring granite (Late Cretaceous)

White- to cream-weathering, highly leucocratic, biotite monzogranite; porphyritic to, less commonly, equigranular. Alkali feldspar megacrysts, as much as 3 cm long, are typically perthitic, euhedral, and white. Much of granite is variably foliated, cataclastic, and recrystallized; locally protomylonitic. Alkali feldspar phenocrysts are converted to augen porphyroclasts. Granite is cut by pegmatite and aplite dikes. Unit makes up much of the southern Quitobaquito Hills, including area of Quitobaquito Springs (Carruth, 1996). In most places Aquajita Spring granite and Paleoproterozoic gneiss (unit Xg) are separated by a minor thrust fault, but on either side of the fault granite locally intrudes gneiss (Haxel et al., 1984; Tosdal et al., 1990). U-Pb zircon age is 80 ± 3 Ma (Rossi, 2022; Rossi et al., 2023). Unit extends southward into northern Sonora, where U-Pb zircon age ≈ 80 Ma was determined by T.H. Anderson (Anderson and Roldan-Quintana, 1979).

As previously noted, Late Cretaceous granitoids as old as 80 Ma are uncommon in southwest Arizona. The only other probable example near OPCMN makes up the entirety of the Alvarez Mountains (Fig. 1). This granite (undated) is unlike rocks in any of the adjacent ranges but petrographically and geochemically similar to the Aquajita Spring granite of OPCMN (although granite in the Alvarez Mountains is more consistently and pervasively foliated).

Late Cretaceous Plutonic and Volcanic Rocks

The three units Kg, Kb, and Kv are closely related, and representative of Late Cretaceous ("Laramide") calcalkaline, metaluminous magmatism (Table 2) in south-central Arizona.

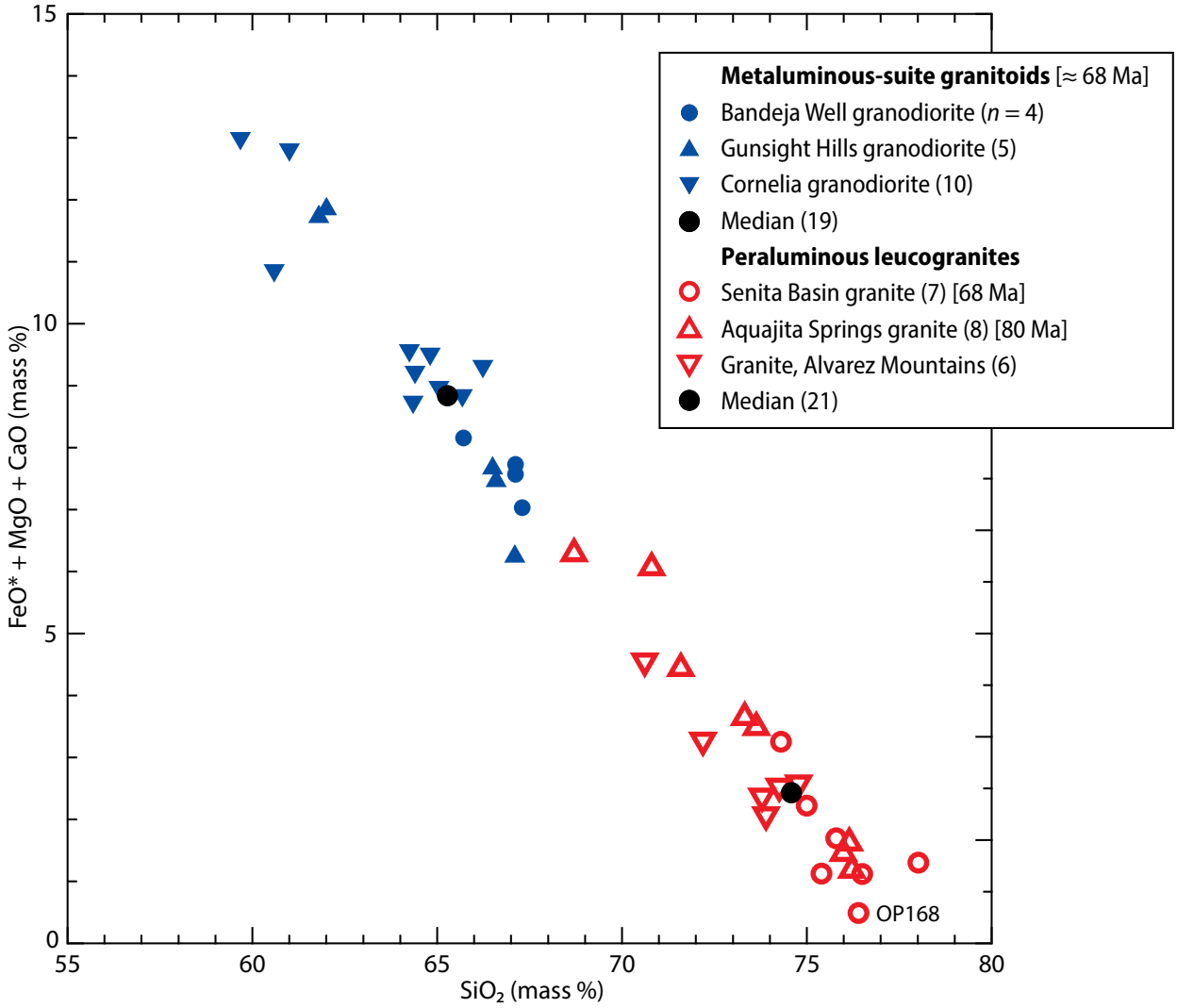


Figure 12. Compositional contrast of OPCNM Late Cretaceous granitoids: calcalkaline, metaluminous, compositionally expanded granodiorite and granite (Haxel et al., 2022); and peraluminous leucogranite. Data plotted include analyses of two units outside OPCMN that have affinities to units within the Monument: Cornelia granodiorite at Ajo; and granite in the Alvarez Mountains (Fig. 1), petrographically and geochemically similar to the Aquajita Spring granite (text). The Aquajita Spring and Senita Basin granites, though similar in composition, are different ages and unrelated. Negative correlation of SiO_2 and FeO* + MgO + CaO owes in part to closure (constant-sum effect). FeO*, total iron as FeO.

Kb Bandeja Well granodiorite (latest Cretaceous)

Gray, leucocratic, hornblende-bearing biotite granodiorite, biotite monzogranite, aplite porphyry, and uncommon titanite-bearing diorite and biotite-hornblende quartz monzonite. Textures are porphyritic to hypidiomorphic-granular to equigranular. Phenocrysts are subhedral to euhedral oligoclase, locally myrmekitic; anhedral, poikilitic, weakly perthitic alkali feldspar; quartz, hornblende, and biotite. Alkali feldspar has myrmekite reaction rims where in contact with oligoclase. Biotite is mostly pseudohexagonal-columnar rather than tabular or platy in habit (Fig. 14), a distinctive and widespread (if inconstant) feature of Late Cretaceous (main "Laramide") granitoid rocks in south-central Arizona (c.f. unit Kg). (This form is colloquially called "stack biotite" or "stacked biotite".) Hornblende is subhedral to euhedral. Accessory minerals include iron oxide (magnetite?), titanite, apatite, and zircon. In most thin sections, titanite is especially abundant. Unit crops out mainly around Growler Pass. The Bandeja Well stock may be the root zone of the porphyry Cu-Mo-Au hydrothermal ore system at Ajo (Gilluly, 1946), ≈ 16 km to the north (Fig. 1); the two having been separated by displacement on Oligocene to Miocene low-angle normal faults (Cox et al., 2006).







Figure 13. Senita Basin granite (unit Ks). **(A)** Typical outcrops, Senita Basin, northern Sonoyta Mountains. (With three species of columnar cacti: organpipe, senita, and saguaro.) **(B)** Inclusion of old phase (beneath and above hammer handle) within young phase. Old phase is medium grained and foliated; young phase coarse grained to pegmatitic and unfoliated. **(C)** Young-phase pegmatite dike in old-phase granite. Hammer 37 cm.

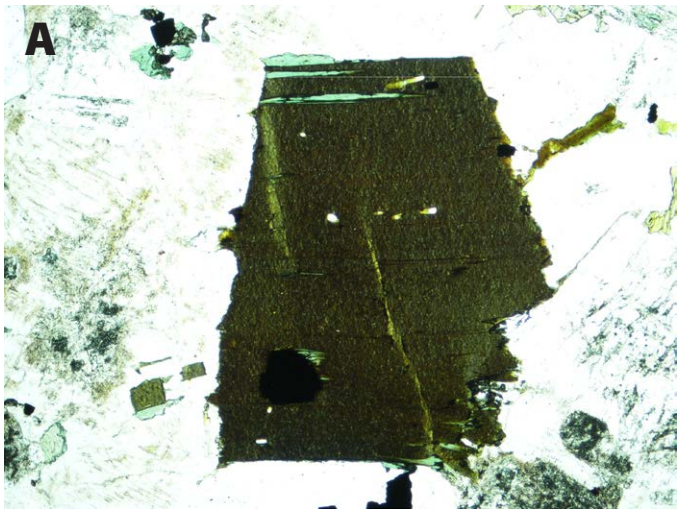




Figure 14. Columnar ("stack") biotite in two samples of Bandeja Well granodiorite. These biotite crystals, view approximately orthogonal to basal cleavage, have height greater than width. **(A)** Crossed polarizers; matrix overexposed; width of view 3.1 mm. **(B)** Plane-polarized light; 6.2 mm. Biotite crystal is strained. Yellow mineral is stained K feldspar.

Kg Gunsight Hills granodiorite (latest Cretaceous)

Light- to medium-gray, medium-grained, porphyritic hornblende-biotite granodiorite, and subordinate biotite leucogranodiorite, intruded by dikes of biotite monzogranite and aplite (Tosdal et al., 1986). Phenocrysts are oligoclase and, less commonly, alkali feldspar. Biotite is generally tabular, but locally has columnar habit like that in Bandeja Well granodiorite (unit Kb). Accessory minerals are titanite, apatite, and zircon. Microscopic recrystallization and deformation textures are common. Local protomylonitic granodiorite gneiss is transitional to unit KP_Ecp. In more deformed rocks, brown igneous biotite is largely recrystallized to green sagenitic biotite. Slightly discordant U-Pb zircon ages are ≈ 67 Ma. Similar granodiorite in the Cimarron Mountains (Fig. 1) has concordant U-Pb zircon age 68 ± 1 Ma (J.E. Wright, *in* Haxel et al., 2022).

Kv Volcanic rocks (Late Cretaceous)

Light-gray to greenish-gray to pinkish-gray silicified flows and tuffs ranging in original composition from andesite to rhyolite. These volcanic to metavolcanic rocks comprise largely secondary minerals: albite, sericite, chlorite, and quartz. Minor relict primary minerals include plagioclase, hornblende, and alkali feldspar; and accessory apatite, zircon, titanite, and magnetite. Unit crops out in the southernmost Growler and northern Bates Mountains, where it is intruded by Bandeja Well granodiorite (unit Kb), to which the volcanic rocks are probably related. Unit probably is broadly correlative with the Concentrator Volcanics, U-Pb zircon age 71.6 ± 0.6 Ma, in the Ajo district 15 km to the north (Gilluly, 1946; Wilkinson, 1998; Cox et al., 2006).

Latest Jurassic Conglomerate

Jc Scarface Mountain conglomerate

Lithic-rich conglomerate and sedimentary breccia containing subangular to subrounded pebbles and cobbles of (originally) quartz arenite, limestone, calcareous siltstone, and granite. Sedimentary-rock clasts are derived largely or entirely from Paleozoic strata of units Cba and DMme. Crops out southeast (Fig. 15) and northeast of Scarface Mountain and in northern Bates Mountains. Basal depositional contact is unconformable: at Lime Hill conglomerate lies on Devonian and Mississippi strata (unit DMme), whereas 2 km to the south it rests on Cambrian rocks (unit Cba). Unit is probably correlative with the latest Jurassic (to earliest Cretaceous?) Glance Conglomerate of southeast and south-central Arizona (e.g., Dickinson and Lawton, 2001; Bassett and Busby, 2005; Haxel 2008a).

Around Scarface Mountain, conglomerate clasts and matrix have been converted to coarse-grained wollastonite-bearing calcsilicate granofels by contact metamorphism accompanying



Figure 15. Metamorphosed latest Jurassic conglomerate (unit Jc), southeast of Scarface Mountain and south of Lime Hill.



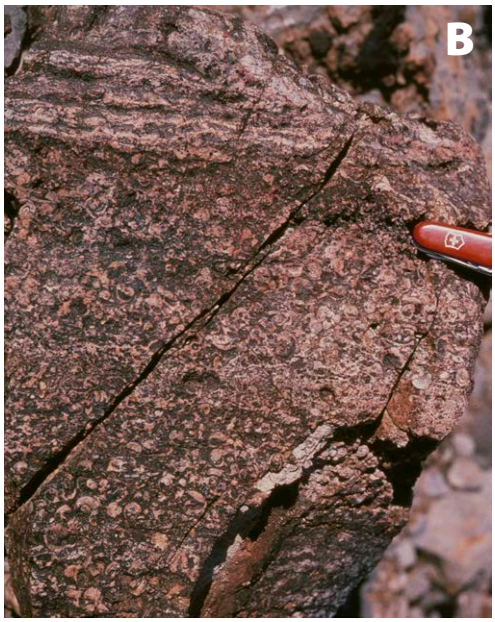


Figure 16. Unmetamorphosed limestone-clast conglomerate (unit Jc, probably), upper San Cristobal Wash drainage, near west-central boundary of OPCNM. **(A)** Dominant pebbles and cobbles of gray limestone. Hammer 37 cm. **(B)** Gastropod fossil hash in clast of Paleozoic, probably Devonian, limestone. Width of image ≈ 24 cm.

intrusion of the latest Cretaceous Bandeja Well granodiorite (unit Kb). Conglomerate is locally intruded by thicker rhyolitic dikes (Miocene?) with vitrophyric margins, and thinner granitic dikes (latest Cretaceous?).

Well-indurated but unmetamorphosed conglomerate and sedimentary breccia containing abundant pebbles and cobbles of Paleozoic limestone (Fig. 16A) crop out in the upper San Cristobal Wash drainage near the west-central boundary of OPCNM (southwest of Bates Mountains, northwest of Cipriano Hills). This rock is provisionally mapped as unit Jc because of its similarity to the Scarface Mountain conglomerate before contact metamorphism. Alternatively but less likely, the conglomerate in the upper San Cristobal Valley could be Cenozoic, possibly related to the Locomotive Canglomerate of the Ajo district (Gilluly, 1946; Cox et al., 2006).

A few of the limestone clasts in the upper San Cristobal conglomerate and breccia are fossiliferous, bearing the only bedrock megafossils known within the Monument (KellerLynn, 2022). The clast shown in Figure 16B contains gastropods that are ". . . likely mid-Paleozoic, but could span between middle Ordovician through Devonian (maybe into Mississippian)." (R.B. Blodgett and V. L. Santucci, NPS, written communication, 2023). Ordovician and Silurian strata are absent from southwest and south-central Arizona (Nations and Stump, 1996), so the limestone clast is probably Devonian. Other clasts contain crinoid stems and unidentified shelly fragments, possibly brachiopods.

Late Jurassic Intrusive Rocks

Diverse plutonic and hypabyssal rocks characterized by outcrop- to hillside-scale heterogeneity. Probably related to the Late Jurassic Ko Vaya Suite that makes up several ranges to the east, particularly North and South Comobabi Mountains and adjacent ranges (Fig. 1; Tosdal et al., 1989; Beikman et al., 1995; Haxel et al., 2008a). The Ko Vaya Suite is imprecisely dated, but U-Pb interpreted ages are ≈ 160–145 Ma, mostly in the younger part of this age range. We presume, provisionally, that the similar (but undated) rocks in OPCMN likewise are Late Jurassic. If this presumption is correct, these Late Jurassic intrusive rocks and the structurally overlying and interleaved Middle Jurassic igneous rocks (units Ja) are 10–20 m.y. different in age and therefore unrelated.

Jr Intrusive rhyolite

Aphanitic, leucocratic hypabyssal rhyolite forming dikes and lenticular bodies within, and presumably related to, heterogeneous granitoid rocks of unit Jh. Exposed in northern Puerto Blanco Mountains and Agua Dulce Mountains (west of map area).

Jh **Acuna Well granite**

Heterogeneous, altered granitic rocks: generally equigranular, leucocratic, coarse-grained to aplitic monzogranite, syenogranite, and alkali feldspar granite; subordinate hornblende quartz diorite. Textural and compositional heterogeneity is pronounced and characteristic (c.f. Haxel et al., 2008a). Locally porphyritic, with phenocrysts of feldspar and biotite. Pink to red, purple, or gray on fresh surfaces; weathers white, red, green, or brown. Intrudes granodiorite (unit Jg); intruded by rhyolite (Jr) and a few dikes of undetermined composition. Rocks are isotropic to weakly foliated, but locally protomylonitic; grading to mylonite and ultramylonite near shear-zone contact with quartzofeldspathic semischist and phyllite (unit Jas). Mapped in Puerto Blanco Mountains, Quitobaquito Hills, and eastern Agua Dulce Mountains. Many of these granitic rocks, including the sample represented in Table 3, evidently have undergone K metasomatism and/or alkali exchange (c.f. Haxel et al., 2008a).

Jhp Porphyritic phase of Acuna Well granite *

Mapped only in easternmost Agua Dulce Mountains.

Jg Granodiorite and quartz diorite (Late Jurassic)

Heterogeneous unit of equigranular to porphyritic, very-fine- to coarse-grained biotite granodiorite and hornblende diorite, coarse-grained biotite diorite, and medium-grained equigranular hornblende monzonite. Generally unfoliated. Pink to red on fresh surfaces, weathers pink to brown. Crops out in the northern Puerto Blanco Mountains, Quitobaquito Hills, and easternmost Agua Dulce Mountains. Also makes up much of Agua Dulce Mountains west of map area.

La Abra complex; Middle and Late Jurassic Igneous and Sedimentary Protoliths, Late Cretaceous to Early Paleogene metamorphism

A suite of variably metamorphosed supracrustal, hypabyssal, and plutonic rocks having two unrelated characteristics in common: Jurassic protolith ages and Late Cretaceous to early Paleogene regional metamorphism (Fig. 5). Six of the seven mapped units—Japn, Jaq, Jaqm, Jac, Jap, Jas—are Middle Jurassic and closely related to one another; some are intergradational. The seventh unit, Late Jurassic metagranite and metagranodiorite (Jag), is associated with the others only in that it was (is) in proximity and consequently has been affected by the same Late Cretaceous to early Paleogene metamorphic event. Metamorphism of the La Abra complex is related to tectonic burial beneath the crystalline upper plate of the Quitobaquito thrust (Haxel et al., 1984; Rossi, 2022; Rossi et al., 2023; see also Iriondo et al., 2005). In most places La Abra units are separated by mylonitic, synmetamorphic shear zones; but gradational, depositional, or intrusive relations between units are locally preserved. The La Abra complex makes up most of the southwest Puerto Blanco Mountains, northern Quitobaquito Hills, and eastern Aqua Dulce Mountains; and part of the Sonoyta Mountains.

Jag Metagranite and metagranodiorite (Late Jurassic)

Metamorphosed granitoid rocks, protomylonitic or mylonitic, locally cataclastic. Derived from units Jh and Jg. Forms shear-zone–bounded sheets in northern Puerto Blanco Mountains.

Jas Quartzofeldspathic semischist and phyllite, chlorite schist (Middle Jurassic)

Unit comprises two lithologic types, not distinguished on the map (Haxel et al., 1984). (1) Predominant very-fine- to medium-grained sericitic quartzofeldspathic semischist (incipiently metamorphosed sandstone: Williams et al., 1982, p. 512) and lesser phyllite, calcareous in part; with subordinate metaconglomerate and marble. Weathering colors are mainly purplish,- reddish, or brownish-gray. Largely metasedimentary and metavolcaniclastic; locally contains relict quartz or feldspar grains, phenocrystic or detrital. Locally mylonitic. (2) Subordinate fine- to medium-grained, dark-green weathering chlorite schist, with platy chlorite derived from biotite; locally mylonitic.

Marble is rare in the Mesozoic supracrustal rocks of south-central and southwest Arizona. Marble in this unit may be related to that in the Chutum Vaya Complex of the southern Baboquivari Mountains (Fig. 1; Goodwin and Haxel, 1990).

Table 3. Whole-rock analyses of representative samples of Middle and Late Jurassic igneous rocks, Organ Pipe Cactus National Monument, southwest Arizona.

Unit	Metamorphosed quartz porphyry (metadacite) (Jaq)	Pozo Nuevo granite porphyry (Japn)	Acuna Well granite (Jh)
Sample	OP429	PUP53	PUP51
Major-element oxides (mass percent)			
SiO_2	70.7	67.8	73.5
TiO_2	0.39	0.43	0.20
Al_2O_3	13.9	15.1	13.9
Fe_2O_3	2.02	2.17	1.23
FeO	0.44	1.18	0.40
MnO	0.06	0.09	0.02
MgO	0.77	1.22	0.40
CaO	1.04	2.36	0.40
Na_2O	2.57	3.58	2.81
K_2O	5.89	4.03	5.73
P_2O_5	0.12	0.13	0.03
H_2O	0.96	0.90	0.82
CO_2	0.62	0.18	0.03
Σ	99.7	99.5	99.6
Trace elements (µg/g)			
Rb	153	113	248
Sr	220	330	130
Ba	1200	1300	930
V	48	72	24
Co	5.8	7.2	3.6
Ni	8.7	6.3	4.6
Cu	17	7.9	7.1
Zn	55	54	<50
Ga	16	12	12
Pb	24	21	30
F	<100	300	200
Zr	180	140	170
La	62	43	60
Ce	140	110	130
Y	29	22	24

Analytical methods (Baedecker, 1987): wavelength-dispersive x-ray fluorescence, quantitative emission spectroscopy.

Jap Quartzofeldspathic phyllite and semischist (Middle Jurassic)

Quartzofeldspathic phyllite and semischist similar to that of unit Jas, with uncommon metaconglomerate.

Jaq Metamorphosed quartz porphyry (Middle Jurassic)

Fine- to very-fine-grained metamorphosed quartz porphyry (Table 3) derived from volcanic, volcaniclastic, hypabyssal, and sedimentary protoliths of broadly rhyolitic to, less commonly, dacitic composition. Generally schistose, with subordinate but pervasive lineation (Fig. 17) (Haxel et al., 1984; Rossi, 2022); less commonly mylonitic or blastomylonitic, particularly along thrust-fault contacts with adjacent units. Relict quartz phenocrysts (Williams and Burr, 1994), 1–5 mm, are prominent and characteristic. Relict phenocrysts of feldspar, pseudohexagonal biotite, and (less commonly) hornblende are apparent in some thin sections and a few hand specimens. Matrix minerals, largely metamorphic, include quartz, feldspar, muscovite, biotite, and minor chlorite. Outcrop colors are gray or silvery gray, white, light green, brown, or buff. The unit locally includes minor mica-poor quartzofeldspathic paraschist and phyllite (similar to units Jas and Jap); and greenschist (similar to that of unit Jac). Structurally, the unit forms several thrust sheets in the northern Puerto Blanco Mountains and Quitobaquito Hill, and makes up most of the eastern Puerto Blanco Mountains. In the latter area, intercalated greenschist and metaconglomerate are mapped separately (unit Jac). U-Pb zircon age of metarhyolite is 170 ± 4 Ma (Rossi, 2022; Rossi et al., 2023). Regional correlations are described in a previous section (p. 7).

Jac Greenschist and metaconglomerate (Middle Jurassic)

Green biotite-chlorite-epidote schist, probably meta-andesite; metaconglomerate similar to that in units Jas and Jap. Greenschist contains plagioclase porphyroclasts (≤1.5 mm), probably relict phenocrysts; and lithic clasts (≤50 cm) of quartz porphyry and other intermediate to silicic volcanic rocks; in a fine-grained epidote-rich matrix. Protolith is probably andesitic lahars or

mudflows. Locally intercalated within metamorphosed quartz porphyry (unit Jaq) in the southern Puerto Blanco Mountains.

Japn Pozo Nuevo granite porphyry (Middle Jurassic)

Leucocratic biotite granite porphyry and porphyritic biotite granite (Fig. 18; Table 3); variably metamorphosed. Phenocrysts are euhedral to subhedral perthitic alkali feldspar, to 1 cm; sericitized oligoclase; and polycrystalline quartz; in a fine-grained matrix of the same minerals plus biotite. Rock is typically slightly foliated, locally strongly foliated; with common variations in size of white to pink feldspar porphyroclasts. Foliation is variably mylonitic, commonly ultramylonitic near ductile faults bounding thrust sheets (Fig. 7). Intruded by small, scattered aplite dikes. Base of mapped unit includes minor chlorite schist (probably derived from unit Jac) and metamorphosed quartz porphyry (Jaq). Weathers greenish-gray to brown. Crops out in Quitobaquito Hills and in a hill along the Sonoran border 4 km east-southeast of Aquajita Spring. In the latter area, base of thrust sheet of Pozo Nuevo granite porphyry is marked by particularly well-developed and photogenic mylonite (Fig. 19; Bezy et al., 2000, p. 34–35).

Rossi (2022) and Rossi et al. (2023) determined two U-Pb zircon ages, for samples separated by 0.55 km and a few minor faults: 168 ± 6 and 178 ± 6 Ma. These two ages overlap at 172–174 Ma, and composite age for both samples is 173.5 ± 7 Ma. Throughout the Quitobaquito Hills, Pozo Nuevo porphyry is closely associated with metamorphosed quartz porphyry (unit Jaq) (Haxel et al., 1984), suggesting Pozo Nuevo age within the range 170 ± 4 Ma is most likely. Considering both geochronologic and geologic evidence, age of the Pozo Nuevo granite porphyry is probably 172–174 Ma.

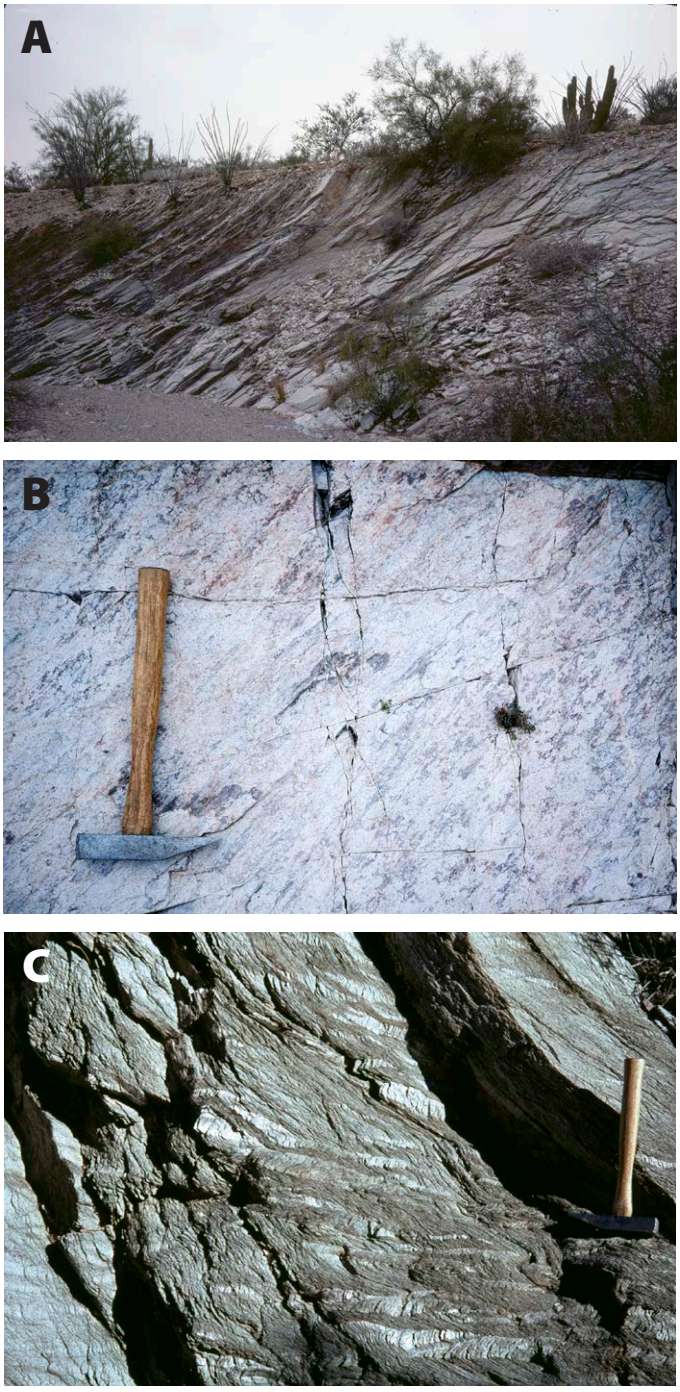


Figure 17. Metamorphosed quartz porphyry (unit Jaq), northern Puerto Blanco Mountains. **(A)** Strongly foliated quartzofeldspathic schist. **(B)** Penetrative lineation, on foliation surface of metamorphosed rhyolite tuff. Grayish objects are recrystallized and stretched pumice pads. **(C)** Crenulation folds (Haxel et al., 1984). Hammer 37 cm

Jaqm Quartzofeldspathic schist derived from metamorphosed quartz porphyry (Middle Jurassic)

This schist forms a dynamothermal aureole on the southwest side of the latest Cretaceous Senita Basin granite (unit Ks) (Haxel et al., 1984; Tosdal et al., 1990). The schist was produced by synplutonic remetamorphism of the metamorphosed quartz porphyry of unit Jaq during intrusion by the Senita Basin granite. Schist is fine to medium grained; gray, tan to orange weathering; and mostly well foliated and lineated. Foliation and lineation



Figure 18. Metamorphosed Pozo Nuevo granite porphyry (unit Japn), Quitobaquito Hills. Knife 9 cm.



Figure 19. Late Cretaceous mylonite derived from Jurassic Pozo Nuevo granite porphyry: porphyroclasts, remnant phenocrysts, of alkali feldspar and quartz in ductilely deformed matrix of quartz, feldspar, chlorite, and relict biotite. Sliced feldspar porphyroclast near center; quartz porphyroclasts (vitreous) right of upper-left edge and above lower edge. Weathered surface subparallel to lineation, approximately orthogonal to foliation. Width of specimen 8–9 cm.

of the same orientation are widespread in southern part of the Senita Basin granite, particularly along its southwest side. Some granite dikes intruding the schist also share this fabric (see unit Ks). Northeast part of the dynamothermal aureole is a mixed zone comprising subequal proportions of quartzofeldspathic schist and granite dikes, some with inclusions of schist.

Paleozoic Sedimentary and Metasedimentary Rocks

Paleozoic cratonal strata crop out in two small areas: at Lime Hill and an unnamed hill 2–2½ km to the south (Fig. 20); and northeast of upper San Cristobal Wash near the west-central boundary of OPCMN. In the latter area, Paleozoic rocks are unmetamorphosed. Around Lime Hill, Paleozoic strata have been contact metamorphosed by intrusion of the latest Cretaceous Bandeja Well granodiorite (unit Kb). Wollastonite is prominent in metamorphosed siliceous limestone (Fig. 21); other metamorphic minerals include calcite, garnet, diopside, and clinozoisite (Reynolds et al., 1988). Paleozoic strata are unconformably overlain by the latest Jurassic Scarface Mountain conglomerate (unit Jc, q.v.; Figs. 15, 20), which contains abundant Paleozoic clasts. Any late Paleozoic or Triassic strata once present in the OPCNM region evidently were eroded before or during latest Jurassic time. Limestone or marble of probable Paleozoic age also crops out in a sliver, several meters long, within the northwest-striking major fault zone separating metamorphosed Jurassic rocks from Neogene volcanic rocks northwest of Pinkley Peak.

DMme Martin Formation and Escabrosa Limestone (Devonian and Mississippian)

Lime Hill area: calcite marble and calcsilicate marble. San Cristobal Wash drainage: limestone and siliceous limestone.

Ꞓba Bolsa Quartzite and Abrigo Formation (Cambrian)

Lime Hill area: quartzite, calcsilicate granofels, calcite marble, and calcsilicate marble.

Paleoproterozoic Igneous and Metamorphic Rocks

Xo Orthogneiss

Several types of orthogneiss, from oldest to youngest: (1) layered biotite quartzofeldspathic gneiss and schist; (2) hornblende-biotite augen gneiss; (3) granitic, typically highly leucocratic, gneiss; (4) amphibolite gneiss; (5) spotted biotite-aggregate granitoid gneiss. Within the map area, restricted to the Quitobaquito Hills, in the upper plate of the Quitobaquito thrust. Here U-Pb zircon age is 1639 ± 37 Ma (Rossi, 2022; Rossi et al.. 2023). Possibly also in part Triassic (c.f. Campbell and Anderson, 2003). Intruded by Late Cretaceous Aquajita Spring granite (unit Ka; q.v.). Unit Xo is allochthonous, having been transported northward (an unknown distance) on the Quitobaquito thrust (Haxel et al., 1984; Rossi, 2022; Rossi et al., 2023). Thus, regional relations of unit Xo, unknown, are more likely to rocks in northwest Sonora (e.g. Nourse et al., 2005) rather than southern Arizona.

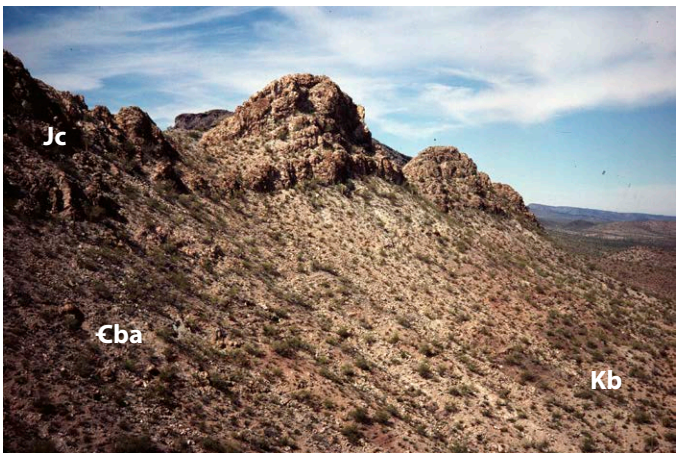


Figure 20. Cambrian Bolsa Quartzite and Abrigo Formation (unit Ꞓba) unconformably overlain by latest Jurassic Scarface Mountain conglomerate (Jc) and underlain by intrusive latest Cretaceous Bandeja Well granodiorite (Kb). Both sedimentary units are contact metamorphosed. Hill southeast of Scarface Mountain and south of Lime Hill.

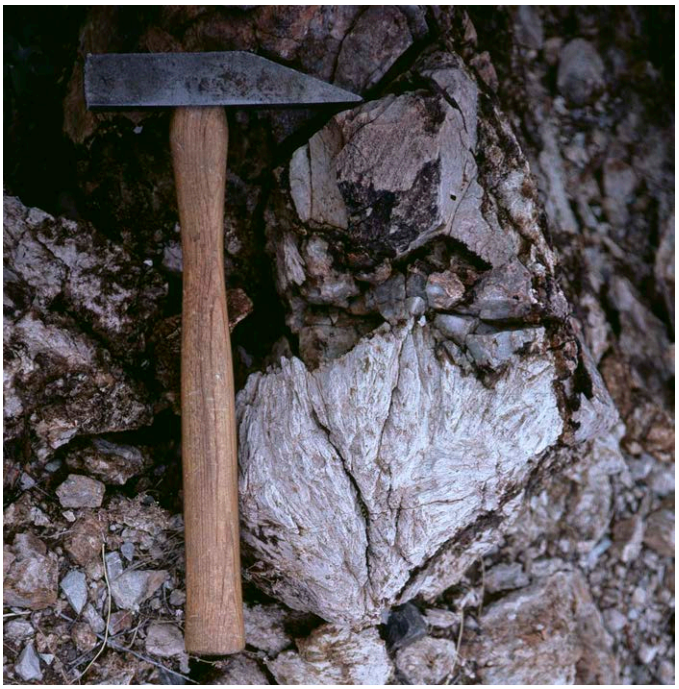


Figure 21. Coarse wollastonite in contact-metamorphic Paleozoic marble (unit DMme). Hammer 37 cm.

Xg Gneiss *

Within the map area restricted to one small, isolated outcrop east of Lime Hill. Presumably similar to some phase of the nearby Paleoproterozoic Cardigan Gneiss, widespread in the Growler Mountains and Little Ajo Mountains (Ajo district) (Gilluly, 1946; Gray et al., 1985; Cox et al., 2006).

Xp Pinal Schist

Fine- to medium-grained biotite and/or muscovite quartzo-feldspathic schist; with generally strong foliation coplanar with lithologic layering, and penetrative lineation in plane of foliation. Restricted to a few small outcrops and shallow artificial depressions south of Lime Hill. This is a local instance of a Paleoproterozoic unit widespread in southern Arizona and northern Sonora (Anderson and Silver, 2005; Meijer, 2014).

ACKNOWLEDGEMENTS

Geologic mapping of Organ Pipe Cactus National Monument, in 1980, was possible only because of support from Terry Peters and Bill Werrell of the National Park Service. Studies of the Jurassic geology of southwest Arizona, including OPCMN, ca. 1978–2008, by Haxel, Tosdal, and May benefited greatly from collaboration with Tom Anderson (University of Pittsburgh). Nancy Riggs (Northern Arizona University) likewise helped us understand the Jurassic paleogeography of southern Arizona. In the 1990s several of the authors learned about the area extending from the northern part of OPCMN north to Ajo from Dennis Cox and Eric Force (USGS). Andrea Eddy produced an early, ca. 1983, partial compilation of our OPCNM mapping. More recently, Amanda Rossi (University of Wyoming) and Jay Chapman (University of Texas, El Paso) shared results of their geochronologic and geologic studies in the Quitobaquito Hills and Sonoyta Mountains. Finally, thanks to Sue Beard and Carson Richardson for thoughtful reviews.

REFERENCES CITED

Anderson, J.L., 1989, Proterozoic anorogenic granites of the southwestern United States, *in* Jenney, J.P., and Reynolds, S.J., eds., Geologic evolution of Arizona: Arizona Geological Society Digest 17, p. 211–238.

Anderson, J.L., and Bender, E.E., 1989, Nature and origin of Proterozoic A-type granitic magmatism in the southwestern United States of America: Lithos, v. 23, p. 19–52.

Anderson, T.H., and Roldan-Quintana, J., eds., 1979, Geology of northern Sonora, Guidebook Field Trip #27, 1979 Annual Meeting of the Geological Society of America: Instituto de Geología. U.N.A.M., Hermasillo, Sonora, Mexico, and University of Pittsburgh, Pittsburgh, Pennsylvania.

Anderson, T.H., and Silver, L.T., 2005, The Mojave-Sonora megashear—Field and analytical studies leading to the conception and evolution of the hypothesis, *in* Anderson, T.H., Nourse, J.A., McKee, J.W., and Steiner, M.B., eds., The Mojave-Sonora megashear hypothesis: Development, assessment, and alternatives: Geological Society of America Special Paper 393, p. 1–50.

Anderson, T.H., Nourse, J.A., McKee, J.W., and Steiner, M.B., eds., 2005a, The Mojave-Sonora megashear hypothesis: Development, assessment, and alternatives: Geological Society of America Special Paper 393, 712 p.

Anderson T.H., Rodríguez-Castañeda, J.L., and Silver, L.T., 2005b, Jurassic rocks in Sonora, Mexico: relations to Mojave-Sonora megashear and its inferred northwestward extension, *in* Anderson, T.H., Nourse, J.A., McKee, J.W., and Steiner, M.B., eds., The Mojave-Sonora megashear hypothesis: Development, assessment, and alternatives: Geological Society of America Special Paper 393, p. 51–95.

Anderson, T.H., and Nourse, J.A., 2005b, Pull-apart basins at releasing bends of the sinistral Late Jurassic Mojave-Sonora fault system, *in* Anderson, T.H., Nourse, J.A., McKee, J.W., and Steiner, M.B., eds., The Mojave-Sonora megashear hypothesis: Development, assessment, and alternatives: Geological Society of America Special Paper 393, p. 97–122.

Baedecker, P.A., ed., Methods for geochemical analysis: U.S. Geological Survey Bulletin 1770, 132 p.

Barton, M.D., Staude, J.-M.G., Zürcher, L., and Megaw, P.K.M., 1995, Porphyry copper and other intrusion-related mineralization in Mexico, *in* Pierce, F.W., and Bolm, J.G., eds., Porphyry copper deposits of the American Cordillera: Arizona Geological Society Digest, v. 20, p. 487–524.

Bau, M., 1996, Controls on the fractionation of isovalent trace elements in magmatic and aqueous systems: evidence from Y/Ho, Zr/Hf, and lanthanide tetrad effect: Contributions to Mineralogy and Petrology, v. 123, p. 323–333

Bassett, K.N., and Busby, C.J., 2005, Tectonic setting of the Glance Conglomerate along the Sawmill Canyon fault zone, southern Arizona: A sequence analysis of an intra-arc strike-slip basin, *in* Anderson, T.H., Nourse, J.A., McKee, J.W., and Steiner, M.B., eds., The Mojave-Sonora megashear hypothesis: Development, assessment, and alternatives: Geological Society of America Special Paper 393, p. 377–400.

Beikman, H.M., Haxel, G.B., and Miller, R.J., 1995, Geologic map of the Tohono O'Odham Indian Nation, southern Arizona: U.S. Geological Survey Miscellaneous Geologic Investigations Map I-2017, scale 1:125,000.

Bennett, S.E.K., and Oskin, M.E., 2014, Oblique rifting ruptures continents: Example from the Gulf of California shear zone: Geology, v. 42, p. 215–218.

Beus, S.S., and and Morales, M., 2003, Grand Canyon geology (2nd ed.): Oxford, 432 p.

Beus, S.S., 1989, Devonian and Mississippian geology of Arizona, *in* Jenney, J.P., and Reynolds, S.J., eds., Geologic evolution of Arizona: Arizona Geological Society Digest 17, p. 287–311.

Bezy, J.V., Gutmann, J. and Haxel, G.B., 2000, A guide to the geology of Organ Pipe Cactus National Monument and the Pinacate Biosphere Reserve: Arizona Geological Survey Down-to-Earth #9, 66 p.

Bilodeau, W.L., Kluth, C.F., and Vedder, L.K., 1987, Regional stratigraphic, sedimentologic, and tectonic relationships of the Glance Conglomerate in southeastern Arizona, *in* Dickinson, W.R., and Klute, M.A., eds., Mesozoic rocks of southern Arizona and adjacent areas: Arizona Geological Society Digest, v. 18, p. 229–256.

Blacet, P.M., Bergquist, J.R., and Miller, S.T., 1978, Reconnaissance geologic map of the Silver Reef Mountains quadrangle, Pinal and Pima County, Arizona: U.S. Geological Survey Miscellaneous Field Studies Map MF-934, scale 1:62,500.

Blakey, R.C., and Ranney, W.D., 2018, Ancient landscapes of western North America: A geologic history with paleogeographic maps: Springer, 228 p.

Bowles, Z., and Greeley, R., 2013, Reconnaissance volcanic geology of the Batamote Mountains, Ajo, Arizona: Journal of the Arizona-Nevada Academy of Science, v. 45(1), p. 37–51.

Brown, J. L. 1992. Interpretive geologic map of Mt. Ajo quadrangle, Organ Pipe Cactus National Monument, Arizona: U.S. Geological Survey Open-File Report 92-23, 15 p., scale 1:24,000.

Busby, C.J., and Centeno-García, E., 2022, The "Nazas Arc" is a continental rift province: Implications for Mesozoic tectonic reconstructions of the southwest Cordillera, U.S. and Mexico: Geosphere, v. 18, p. 647–669.

Busby, C.J., Bassett, K., Steiner, M.B., and Riggs, N.R., 2005, Climatic and tectonic controls on Jurassic intra-arc basins related to northward drift of North America, *in* Anderson, T.H., Nourse, J.A., McKee, J.W., and Steiner, M.B., eds., The Mojave-Sonora megashear hypothesis: Development, assessment, and alternatives: Geological Society of America Special Paper 393, p. 359–376.

Busby-Spera, C.J., 1988, Speculative tectonic model for the early Mesozoic arc of the southwest Cordilleran United States: Geology, v. 16, p. 1121–1125.

Campbell, P.A., and Anderson, T.H., 2003, Structure and kinematics along a segment of the Mojave-Sonora megashear: A strike-slip fault that truncates the Jurassic continental magmatic arc of southwestern North America: Tectonics, v. 22, no. 6, p. 1077–1098.

Carrigan, F.J., 1971, A geologic investigation of contact metamorphic deposits in the Coyote Mountains, Pima County, Arizona: University of Arizona, M.S. thesis, 67 p.

Carruth, R.L., 1996, Hydrogeology of the Quitobaquito Springs and La Abra Plain, Arizona, Organ Pipe Cactus National Monument, and Sonora, Mexico: U.S. Geological Survey Water-Resources Investigations Report 95-4295, 23 p.

Černý, P., Meintzer, R.E., and Anderson, A.J., 1985, Extreme fractionation in rare-element granitic pegmatites: selected examples of data and mechanisms: Canadian Mineralogist, v. 23, p. 381–421.

Chapman, J.B., Runyon, S.E., Shields, J.E., Lawler, B.L., Pridmore, C.J., Scoggin, S.H., Swaim, N.T., Trzinski, A.E., Wiley, H.N., Barth, A.P. and Haxel, G.B., 2021, The North American Cordilleran anatectic belt: Earth-Science Reviews, v. 215, 103576.

Chapman, J.B., Pridmore, C., Chamberlain, K., Haxel, G.B., and Ducea, M., 2023, Himalayan-like crustal melting and differentiation in the southern North American Cordilleran anatectic belt during the Laramide orogeny: Coyote Mountains, Arizona: Journal of Petrology, v. 64, p. 1–22.

Cox, D.P., Force, E.R., Wilkinson, W.H., More, S.W., Rivera, J.S., and Wooden, J.L., 2006, The Ajo mining district, Pima County, Arizona: Evidence for mid-Tertiary detachment faulting, plutonism, volcanism, and hydrothermal alteration: U.S. Geological Survey Professional Paper 1733, 46 p.

Dickinson, W.R., 1989, Tectonic setting of Arizona through geologic time, *in* Jenney, J.P., and Reynolds, S.J., eds., Geologic evolution of Arizona: Arizona Geological Society Digest 17, p. 1–16.

Dickinson, W.R., and Lawton, T.F., 2001, Tectonic setting and sandstone petrofacies of the Bisbee Basin (USA-Mexico): Journal of South American Earth Sciences, v. 14, p. 475–504.

Dimmitt, M.A., Comus, P.W., and Brewer, L.M., 2015, A natural history of the Sonoran Desert (second edition): Arizona-Sonora Desert Museum Press and University of California Press, 575 p.

Dockter, R. D., and Keith, W. J., 1978, Reconnaissance geologic map of the Vekol Mountains 15-minute quadrangle, Arizona: U.S. Geological Survey Miscellaneous Field Studies Map MF-931, scale 1:62,500.

Eberly, L.D. and Stanley Jr., T.B., 1978, Cenozoic stratigraphy and geologic history of southwestern Arizona: Geological Society of America Bulletin, v. 89, p. 921–940.

Fackler-Adams, B.N., Busby, C.J., and Mattinson, J.M., 1997, Jurassic magmatism and sedimentation in the Palen Mountains, southeastern California: Implications for regional tectonic controls on the Mesozoic arc: Geological Society of America Bulletin, v. 109, p. 1464–1484.

Felger, R.S., Warren, P. L., Anderson, L.S., and Nabhan, G. P. , 1992, Vascular plants of a desert oasis: Flora and ethnobotany of Quitobaquito, Organ Pipe Cactus National Monument, Arizona: Proceedings of the San Diego Society of Natural History, no. 8, p. 1–39.

Felger, R.S., Broyles, B., Wilson, M.F., Nabhan, G.P., and Turner, D.S., 2007, Six grand reserves, one grand desert, *in* Felger, R.S., and Broyles, B., eds., Dry borders: Great natural reserves of the Sonoran Desert: Utah, p. 3–26.

Gilluly, J., 1946, The Ajo mining district, Arizona: U. S. Geological Survey Professional Paper 209, 112 p.

Goodwin, L.B., and Haxel, G.B., 1990, Structural evolution of the southern Baboquivari Mountains, south-central Arizona and north-central Sonora: Tectonics, v. 9, p. 1077–1095.

Gray, F. and Miller, R.J., 1984a, New K-Ar Age of volcanic rocks near Ajo, Pima and Maricopa Counties, southwestern Arizona: Isocron/West Bulletin of Isotopic Geochronology, no. 41, p. 3–6.

Gray, F. and Miller, R.J., 1984b, Stratigraphy, geochronology, and geochemistry of a calc-alkaline volcanic field near Ajo, southwestern Arizona: Geological Society of America Abstracts with Programs, v. 16, no. 6, p. 3–6.

Gray, F., Miller, R.J., Grubensky, M.J., Tosdal, R.M., Haxel, G.B., Peterson, D.W., May, D.J., and Silver, L.T., 1988, Geologic map of the Ajo and Lukeville 1°-by-2° quadrangles, southwestern Arizona: U.S. Geological Survey Open-File Report 87-0347, scale 1:250,000, 23 p.

Gray, F., Miller, R.J., Peterson, D.W., May, D.J., Tosdal, R.M., and Kahle, K., 1985, Geologic map of the Growler Mountains, Pima and Maricopa Counties, Arizona: U.S. Geological Survey Miscellaneous Field Studies Map MF-1681, scale 1:62,500.

Greig, R.E., and Barton, M.D., 2019, Regional-scale evolution of the Laramide arc and porphyry copper province, southwestern North America, *in* Pearthree, P.A., ed., Geologic Excursions in southwestern North America: Geological Society of America Field Guide 55, p. 401–406.

Haxel, G.B., May, D.J., Wright, J.E., and Tosdal, R.M., 1980a, Reconnaissance geologic map of the Baboquivari Peak 15′ quadrangle, Arizona: U.S. Geological Survey Miscellaneous Field Studies Map MF-1251, scale 1:62,500.

Haxel, G.B., Wright, J.E., May, D.J., and Tosdal, R.M., 1980b, Reconnaissance geology of the Mesozoic and lower Cenozoic rocks of the southern Papago Indian Reservation, Arizona: A preliminary report, *in* Jenny, J.P., and Stone, C., eds., Studies in western Arizona: Arizona Geological Society Digest 12, p. 17–29.

Haxel, G.B., Tosdal, R.M., May, D.J., and Wright, J.E., 1984, Late Cretaceous and early Tertiary orogenesis in south-central Arizona: thrust faulting, regional metamorphism, and granitic plutonism: Geological Society of America Bulletin, v. 95, p. 631–653.

Haxel, G.B., Wright, J.E., Riggs, N.R., Tosdal, R.M., and May, D.J., 2005, Middle Jurassic Topawa Group, Baboquivari Mountains, south-central Arizona: volcanic and sedimentary record of deep basins within the Jurassic magmatic arc, *in* Anderson, T.H., Nourse, J.A., McKee, J.W., and Steiner, M.B., eds., The Mojave-Sonora megashear hypothesis: Development, assessment, and alternatives: Geological Society of America

Special Paper 393, p. 329–357.

Haxel, G.B., Anderson, T.H., Briskey, J.A., Tosdal, R.M., Wright, J.E., and May, D.J., 2008a, Late Jurassic igneous rocks in south-central Arizona and north-central Sonora: Magmatic accompaniment of crustal extension, *in* Spencer, J.E., and Titley, S.R., eds., Ores and orogenesis: Circum-Pacific tectonics, geologic evolution, and ore deposits: Arizona Geological Society Digest 22, p. 333–355.

Haxel, G.B., May, D.J., Anderson, T.H., Tosdal, R.M., and Wright, J.E., 2008b, Geology and geochemistry of Jurassic plutonic rocks, Baboquivari Mountains, south-central Arizona, *in* Spencer, J.E., and Titley, S.R., eds., Ores and orogenesis: Circum-Pacific tectonics, geologic evolution, and ore deposits: Arizona Geological Society Digest 22, p. 497–515.

Haxel, G.B., Johnson, D.A., Briskey, J.A., Tosdal, R.M. and Wright, J.E., 2022, Ore and other metals in Laramide metaluminous and peraluminous granitoids, and in the upper crust, south-central Arizona and north-central Sonora: Arizona Geological Survey Contributed Report CR-22-D, 45 p.

Iriondo, A., Martínez-Torres, L.M., Kunk, M.J., Atkinson, W.W., Jr., Premo, W.R., and McIntosh, W.C., 2005, Northward Laramide thrusting in the Quitovac region, northwestern Sonora, Mexico: Implications for the juxtaposition of Paleoproterozoic basement blocks and the Mojave-Sonora megashear hypothesis, *in* Anderson, T.H., Nourse, J.A., McKee, J.W., and Steiner, M.B., eds., The Mojave-Sonora Megashear hypothesis: Development, assessment, and alternatives: Geological Society of America Special Paper 393, p. 631–669.

Jones, W.C., 1974, General geology of the northern portion of the Ajo Range, Pima County, Arizona: University of Arizona, M.S. Thesis, 77 p.

Karlstrom, K.E. and Bowring, S.A., 1988, Early Proterozoic assembly of tectonostratigraphic terranes in southwestern North America: Journal of Geology, v. 96, no. 5, p. 561–576.

Keith, S.B., 1974, Index of mining properties in Pima County, Arizona: Arizona Bureau of Mines Bulletin 189, 156 p.

KellerLynn, K. 2022. Organ Pipe Cactus National Monument: Geologic resources inventory report. Natural Resource Report NPS/NRSS/GRD/NRR—2022/2399: National Park Service, Fort Collins, Colorado. https://doi. org/10.36967/2293664.

Łabaj, M.A., and Pratt, B.R., 2016, Depositional dynamics in a mixed carbonate-siliciclastic system: Middle–Upper Cambrian Abrigo Formation, southeastern Arizona, U.S.A.: Journal of Sedimentary Research, v. 86, p. 11–37.

Lang, J.R., and Titley, S.R., 1998, Isotopic and geochemical characteristics of Laramide magmatic systems in Arizona and implications for the genesis of porphyry copper deposits: Economic Geology, v. 93, p. 138–170.

Laird, W., Murrieta-Saldivar, J., and Shepard, J., 1997, Cooperation across the border: A brief history of biosphere reserves in the Sonoran Desert, *in* Felger, R.S., and Broyles, B., eds., Dry borders: Journal of the Southwest, v. 39, no. 3–4, p. 307–313.

May, D.J., Peterson, D.W., Tosdal, R.A., LeVeque, R.A., and Miller, R.J., 1981, Miocene volcanic rocks of the Ajo Range, south central Arizona: *in* Howard, K.A., Carr, M.D., and Miller, D.M., eds., Tectonic framework of the Mojave and Sonoran Deserts, California and Arizona: U.S. Geological Survey Open File Report 81-503, p. 65–66.

McKee, E.D., 1947, Paleozoic seaways in western Arizona: American Association of Petroleum Geologists Bulletin, v. 31, p. 282–292.

Meijer, A., 2014, The Pinal Schist of southern Arizona: A Paleoproterozoic forearc complex with evidence of spreading ridge–trench interaction at ca. 1.65 Ga and a Proterozoic arc obduction event: Geological Society of America Bulletin, v. 126, p. 1145–1163.

Middleton, L.T.,1989, Cambrian and Ordovician depositions systems in Arizona, *in* Jenney, J.P., and Reynolds, S.J., eds., Geologic evolution of Arizona: Arizona Geological Society Digest 17, p. 273–286.

Nations, D., and Stump, E., 1996, Geology of Arizona (2nd ed.): Kendall/Hunt, 260 p.

Nourse, J.A., Anderson, T.H., and Silver, L.T., 1994, Tertiary metamorphic core complexes in Sonora, northwestern Mexico: Tectonics, v. 13, p. 1161–1182.

Nourse, J.A., Premo, W.R., Iriondo, A., and Stahl, E.R., 2005, Contrasting Proterozoic basement complexes near the truncated margin of Laurentia, northwestern Sonora–Arizona international border region, *in* Anderson, T.H., Nourse, J.A., McKee, J.W., and Steiner, M.B., eds., The Mojave-Sonora megashear hypothesis: Development, assessment, and alternatives: Geological Society of America Special Paper 393, p. 123–182.

Pearthree, P.A., Youberg, A., and Young, J.J., 2020, Geologic map of the Tillotson Peak 7½′ quadrangle and part of the Mount Ajo 7½′ quadrangle, Organ Pipe Cacuts National Monument, Pima County, Arizona: Arizona Geological Survey Digital Geologic Map DGM-73, v. 2.0, scale 1:24,000.

Pourmand, A., Dauphas , N., and Ireland, T.J., 2012, A novel extraction chromatography and MC-ICP-MS technique for rapid analysis of REE, Sc and Y: Revising CI-chondrite and Post-Archean Australian Shale (PAAS) abundances: Chemical Geology, v. 291, p. 38–54.

Reynolds, S.J., Richard, S.M., Haxel, G.B., Tosdal, R.M., and Laubach, S.E., 1988, Geologic setting of Mesozoic and Cenozoic metamorphism in Arizona, *in* Ernst, W.G., ed., Metamorphism and crustal evolution of the western United States (Rubey Volume 7): Prentice Hall, p. 466–501.

Richard, S.M., Reynolds, S.J., Spencer, J.E., and Pearthree, P.A., compilers, 2000, Geologic map of Arizona: Arizona Geological Survey Map 35, scale 1:1,000,000.

Riggs, N.R., and Busby-Spera, C.J., 1991, Facies analysis of an ancient, dismembered, large caldera complex and implications for intra-arc subsidence: Middle Jurassic strata of Cobre Ridge, southern Arizona, USA: Sedimentary Geology, v. 74, p. 39–68.

Riggs, N.R., and Haxel, G.B., 1990, The Early to Middle Jurassic magmatic arc in southern Arizona: plutons to sand dunes, *in* Gehrels, G.E., and Spencer, J.E., eds., Geologic excursions through the Sonoran Desert region, Arizona and Sonora: Arizona Geological Survey Special Paper 7, p. 90–103.

Riggs, N.R., Mattinson, J.M., and Busby, C.J., 1993, Correlation of Jurassic eolian strata between the magmatic arc and the Colorado Plateau: New U-Pb geochronologic data from southern Arizona: Geological Society of America Bulletin, v. 105, p. 1231–1246.

Rossi, A.M., 2022, Evidence for reverse-sense ductile shear during the Laramide orogeny in southwestern Arizona: Quitobaquito Hills: University of Wyoming, M.S. Thesis, 73 p.

Rossi, A.M., Chapman, J.B., John, B.E., Haxel, G.B., and Iriondo, A., 2023, Evidence for reverse-sense ductile shear during the Laramide orogeny in southwestern Arizona: Quitobaquito Hills, *in* Inriondo, A., Lawton, F.F., Estrada-Carmona, J., Geissman, J.W., Sierra-Rojas, M.I., Rodríguez-Trejo, A., and Böhnel, H., eds., Late Paleozoic to Cenozoic of Mexico and beyond: Stratigraphy, magmatism, geochronology, tectonics, and paleomagnetism: Geological Society of America Special Paper, in press.

Shafiqullah, M., Damon, P.E., Lynch, D.J., Reynolds, S.J., Rehrig, W.A., and Raymond, R.H., 1980, K-Ar geochronology and geologic history of southwestern Arizona and adjacent areas, *in* Jenny, J.P., and Stone, C., eds., Studies in western Arizona: Arizona Geological Society Digest 12, p. 201–242.

Skinner, L.A., Haxel, G.B., and Umhoefer, P.J., 2008, Geological reconnaissance at Organ Pipe Cactus National Monument, Arizona, unpublished digital data: Northern Arizona University, Flagstaff, Arizona, scale 1:24,000. [https://irma.nps.gov/DataStore/Reference/Profile/1049253]

Spencer, J.E., Richard, S.M., Reynolds, S.J., Miller, R.J., Shafiqullah, M., Gilbert, W.G., and Grubensky, M.J., 1995, Spatial and temporal relationships between mid-Tertiary magmatism and extension in southwestern Arizona: Journal of Geophysical Research, v. 100, no. B7, p. 10,321–10,351.

Staude, J.G. and Barton, M.D., 2001, Jurassic to Holocene tectonics, magmatism, and metallogeny of northwestern Mexico: Geological Society of America Bulletin, v. 113, p. 1357–1374.

Tosdal, R.M., and Wooden, J.L., 2015, Construction of the Jurassic magmatic arc, southeast California and southwest Arizona, *in* Anderson, T.H., Didenko, A.N., Johnson, C.L., Khanchuk, A.I., and MacDonald, J.H. Jr., eds., Late Jurassic margin of Laurasia—A record of faulting accommodating plate rotation: Geological Society of America Special

Paper 513, p. 189–221.

Tosdal R.M., Haxel, G.B., and Wright, J.E., 1989, Jurassic geology of the Sonoran Desert region, southern Arizona, southeastern California, and northernmost Sonora: Construction of a continental-margin magmatic arc, *in* Jenney, J.P., and Reynolds, S.J., eds., Geologic evolution of Arizona: Arizona Geological Society Digest 17, p. 397–434.

Tosdal, R.M., Haxel, G.B., Anderson, T.H., Connors, C.D., May, D.J., and Wright, J.E., 1990, Highlights of Jurassic, Late Cretaceous to early Tertiary, and middle Tertiary tectonics, south-central Arizona and north-central Sonora, *in* Gehrels, G.E., and Spencer, J.E., eds., Geologic excursions through the Sonoran Desert region, Arizona and Sonora: Arizona Geological Survey Special Paper 7, p. 76–88.

Tosdal, R.M., Peterson, D.W., May, D.J., LeVeque, R.A., and Miller, R.J., 1986, Reconnaissance geologic map of the Mount Ajo and part of the Pisinimo 15′quadrangles, Pima County, Arizona: U.S. Geological Survey, scale 1:62,500.

Turner, R.M., Bowers, J.E., and Burgess, T.L., 1995, Sonoran desert plants: An ecological atlas: Arizona, 501 p.

Umhoefer, P.J., Dorsey, R.J., Darin, M.H., Bennett, S.E.K., Skinner, L.A., and Oskin, M.E., 2018, Breaching of strike-slip faults and successive flooding of pull-apart basins to form the Gulf of California seaway from ca. 8–6 Ma: Geology, v. 46, p. 695–698.

Wilkinson, W.H., 1998, Geological and structural evolution of the Ajo porphyry copper deposit, Pima County, Arizona [abs.]: Society of Mining Engineers Annual Meeting, March 1–3, 1999, p. 85.

Williams, H., Turner, F.J., and Gilbert, C.M., 1982, Petrography: An introduction to the study of rocks in thin section: Freeman, 626 p.

Williams, M.L., and Burr, J.L., 1994, Preservation and evolution of quartz phenocrysts in deformed rhyolites from the Proterozoic of southwestern North America: Journal of Structural Geology, v. 16, p. 203–221.

Wright, J.E., and Haxel, Gordon, 1982, A garnet-two-mica granite, Coyote Mountains, southern Arizona: Geologic setting, uranium-lead isotopic systematics of zircon, and nature of the granite source region: Geological Society of America Bulletin, v. 93, p. 1176–1188.

Wruke, C.T., 1989, The Middle Proterozoic Apache Group, Troy Quartzite, and associated diabase of Arizona, *in* Jenney, J.P., and Reynolds, S.J., eds., Geologic evolution of Arizona: Arizona Geological Society Digest 17, p. 239–258.

Youberg, A. and Pearthree, P.A., 2020, Geologic map of parts of Lukeville, Diaz Peak, South of Lukeville and Blankenship Wells 7½′ quadrangles, Organ Pipe Cactus National Monument, Pima County, Arizona v 2.0: Arizona Geological Survey Digital Geologic Map DGM-74, scale 1:24,000.

Young, J.J. and Pearthree, P.A., 2020, Geologic map of the Armenta Well 7½′ quadrangle and part of the Gunsight 7½′ quadrangle, Organ Pipe Cactus National Monument, Pima County, Arizona: Arizona Geological Survey Digital Map DGM-72, v 2.0, scale 1:24,000.

UA SCIENCE
ARIZONA GEOLOGICAL SURVEY

Bedrock Geologic Map of Organ Pipe Cactus National Monument and Vicinity, Southwest Arizona

Lisa A. Thompson[1,2], Gordon B. Haxel[2,3,4], Donald W. Peterson[4], Daniel J. May[4], Richard M. Tosdal[4], Robert J. Miller[4], Floyd Gray[4], Richard A. LeVeque[4], Paul J. Umhoefer[3]

Present or recent affiliations:
[1]Arizona Geological Survey, University of Arizona, Tucson, Arizona; [2]U.S. Geological Survey, Flagstaff, Arizona; [3]Division of Geosciences, School of Earth and Sustainability, Northern Arizona University, Flagstaff, Arizona
Affiliation at the time of mapping:
[4]U.S. Geological Survey, Menlo Park, California

CR-24-B
PLATE 1

113°0'0"W
112°50'0"W
112°40'0"W
32°10'0"N
32°0'0"N
31°50'0"N

Legend:

Map Units

Quaternary surficial deposits
- Qg - alluvial deposits, undivided

Neogene to Late Paleogene rocks

Batamote Andesite complex
- Nbu - Flows, flow breccias, and vent intrusive rocks, undivided
- Nba - Basaltic andesite flows and flow breccias
- Nbb - Porphyritic basalt
- Nbai - Vent intrusive rocks
- Nbab - Vent breccias

Montezuma Head rhyolite
- Nmu - Rhyolite, undivided
- Nmat - Crystal-lithic ash-flow tuff
- Nmr - Rhyolite, rhyodacite, and minor dacite flows, flow breccias, and plugs
- Nmt - Tuff and tuff breccia
- Nmb - Porphyritic basalt of Diablo Mountains
- Nmd - Dacite of Ajo Range
- Nma - Augite andesite and hypersthene-hornblende andesite of Ajo Range

Childs Latite and coeval plutonic rocks
- Ncu - Latite and coeval plutonic rocks, undivided
- Ncl - Latite flows and flow breccias
- Nca - Augite andesite
- Ncb - Olivine-augite basalt and alkali basalt
- Ncm - Monzogranite of Siovi Shuatak Wash and related rocks

Pinkley Peak rhyolite
- Npr - Biotite rhyolite domes, flows, agglomerates, and tuffs
- Nprd - Rhyolite, rhyodacite, and dacite flows and flow breccias
- Npt - Lithic lapilli tuff
- Nphd - Hornblende dacite flows and agglomerate
- Nps - Arkosic and volcaniclastic sandstone
- Npa - Augite andesite

Miscellaneous igneous and sedimentary rocks
- Ndc - Daniels Conglomerate and associated lacustrine rocks
- Nh - Hornblende dacite
- Nr - Rhyolite flows, dikes, and pyroclastic rocks
- Nt - Growler Mountain welded tuff
- Nsv - Sedimentary and volcanic rocks
- Nv - Pyroclastic rocks
- P_Ls - Schuchuli granite

Late Cretaceous to Early Paleogene rocks

Chagit Vo gneiss
- KP_Lcb - Blastomylonitic granodiorite gneiss
- KP_Lcp - Protomylonitic granodiorite gneiss

Cretaceous rocks
- Ks - Senita Basin granite
- Kb - Bandeja Well granodiorite
- Kg - Gunsight Hills granodiorite and related rocks
- Kv - Volcanic and metavolcanic rocks
- Ka - Aguajita Spring granite

Jurassic rocks

Sedimentary rocks
- Jc - Scarface Mountain conglomerate

Plutonic rocks
- Jr - Intrusive rhyolite related to Agua Dulce granite
- Jh - Acuna Well granite
- Jhp - Porphyritic phase of Jh
- Jg - Granodiorite and quartz diorite

La Abra complex
- Jag - Metagranite and metagranodiorite
- Jap - Quartzofeldspathic phyllite and semischist
- Jas - Quartzofeldspathic semischist and phyllite chlorite schist
- Jaqm - Quartzofeldspathic schist derived from Jaq
- Jaq - Metaquartz porphyry
- Jac - Greenschist and metaconglomerate
- Japn - Pozo Nuevo granite porphyry

Paleozoic rocks
- DMme - Martin Formation and Escabrosa Limestone
- Cba - Bolsa Quartzite and Abrigo Formation

Proterozoic rocks
- Xo - Orthogneiss
- Xg - Orthogneiss and foliated granite
- Xp - Pinal Schist

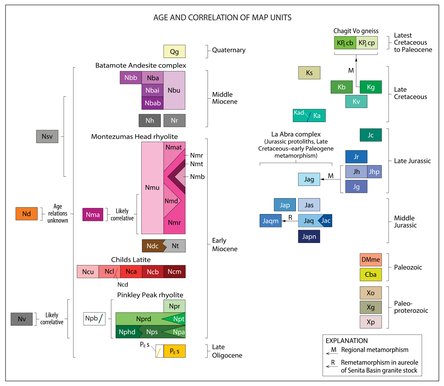
Contacts and Faults
- known contact
- approximate contact
- gradational contact
- anticline, approximate
- anticline, concealed
- thrust fault, known or certain
- normal fault, known or certain
- normal fault, approximate
- normal fault, concealed
- subsidiary thrust, known or certain
- subsidiary thrust, concealed
- subsidiary thrust, approximate and queried
- subsidiary thrust, inferred

Dikes
- Nbai - Batamote Andesite complex, dikes undivided
- Nmu - Rhyolite of Montezumas Head, rhyolite dikes
- Ncd - Childs Latite, augite latite dikes
- Npb - Pinkley Peak rhyolite, olivine-augite basalt dikes
- Nd - Neogene dikes
- P_Ls - Schuchuli granite, syenogranite porphyry dikes
- Kad - Aguajita Spring granite, diabase dike

Geologic orientations
- strike and dip of inclined beds
- horizontal beds
- strike and dip of inclined beds, tops known from sedimentary structures
- strike and dip of inclined foliation
- strike of vertical foliation
- strike and dip of inclined joints
- strike of vertical joints
- trend and plunge of inclined lineation, plunge not labeled
- vertical lineation
- trend and plunge of inclined minor fold axis
- strike and dip of inclined vein
- strike and dip of inclined igneous fabric
- strike and dip of inclined igneous fabric, approximately located

Other symbols
- park boundary
- ephemeral stream
- index contour line
- contour line
- geochronology sample location (map report Table 1)

AGE AND CORRELATION OF MAP UNITS



Age and correlation of map units. Dikes shown as boxes where their lithic designator is different from the host map unit.

SCALE 1:40,000

0 1 2 4 6 8 10
MILES
0 1 2 4 6 8 10
KILOMETERS

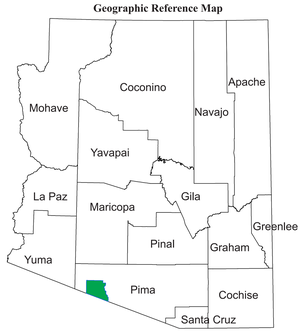
CONTOUR INTERVAL 100 FT

NAD83 UNIVERSAL TRANVERSE MERCATOR ZONE 12N

TOPOGRAPHIC BASE MAP MOSAICKED FROM USGS TOPO MAP VECTOR DATA, 7.5 X 7.5 QUADRANGLES ORIGINALLY IN NAD27 DATUM.
VECTOR DATA PUBLISH DATE 08/07/2018

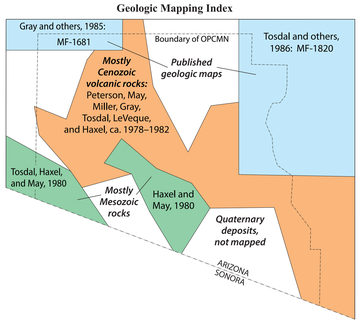
9.90 °E
TN
MN

Geographic Reference Map



Green—location of Organ Pipe Cactus National Monument in southwest Arizona. Counties labeled.

Geologic Mapping Index



Digitial geologic map compilation from: blue rectangles—published geologic maps; green & orange polygons—unpublished mapping; white polygons—Quaternary deposits, not mapped.

References:

Gray, F., Miller, R.J., Peterson, D.W., May, D.J., Tosdal, R.M., and Kahle, K., 1985, Geologic map of the Growler Mountains, Pima and Maricopa Counties, Arizona: U.S. Geological Survey Miscellaneous Field Studies Map MF-1681, scale 1:62,500.

Tosdal, R.M., Peterson, D.W., May, D.J., LeVeque, R.A., and Miller, R.J., 1986, Reconnaissance geologic map of the Mount Ajo and part of the Pisinimo quadrangles, Pima County, Arizona: U.S. Geological Survey Miscellaneous Field Studies Map MF-1820, scale 1:62,500.